

1   **The RopGEF KARAPPO is Essential for the Initiation of**  
2   **Vegetative Reproduction in *Marchantia***

3

4   Takuma Hiwatashi,<sup>1</sup> Koh Li Quan,<sup>2</sup> Yukiko Yasui,<sup>1</sup> Hideyuki Takami,<sup>1</sup> Masataka  
5   Kajikawa,<sup>3</sup> Hiroyuki Kираita,<sup>3</sup> Mayuko Sato,<sup>4</sup> Mayumi Wakazaki,<sup>4</sup> Katsushi Yamaguchi,<sup>5</sup>  
6   Shuji Shigenobu,<sup>5</sup> Hidehiro Fukaki,<sup>1</sup> Tetsuro Mimura,<sup>1</sup> Katsuyuki T. Yamato,<sup>7</sup> Kiminori  
7   Toyooka,<sup>4</sup> Shinichiro Sawa,<sup>6</sup> Daisuke Urano,<sup>2</sup> Takayuki Kohchi,<sup>3</sup> and Kimitsune  
8   Ishizaki,<sup>1,8\*</sup>

9

10   <sup>1</sup>Graduate School of Science, Kobe University, Kobe 657-8501, Japan.

11   <sup>2</sup>Temasek Life Sciences Laboratory, National University of Singapore, Singapore 117604,  
12   Singapore.

13   <sup>3</sup>Graduate School of Biostudies, Kyoto University, Kyoto 606-8502, Japan.

14   <sup>4</sup>RIKEN Center for Sustainable Resource Science, Yokohama 230-0045, Japan.

15   <sup>5</sup>Functional Genomics Facility, National Institute for Basic Biology (NIBB), Okazaki,  
16   Aichi 444-8585, Japan.

17   <sup>6</sup>Graduate School of Science and Technology, Kumamoto University, Kumamoto 860-8555,  
18   Japan.

19   <sup>7</sup>Faculty of Biology-Oriented Science and Technology, Kindai University, Kinokawa,  
20   Wakayama 649-6493, Japan.

21   <sup>8</sup>Lead Contact

22   \*Correspondence: kimi@emerald.kobe-u.ac.jp (K.I.)

23

24

25 **SUMMARY**

26 Many plants can reproduce vegetatively, producing clonal progeny from vegetative cells;  
27 however, little is known about the molecular mechanisms underlying this process.  
28 Liverwort (*Marchantia polymorpha*), a basal land plant, propagates asexually via gemmae,  
29 which are clonal plantlets formed in gemma cups on the dorsal side of the vegetative  
30 thallus [1]. The initial stage of gemma development involves elongation and asymmetric  
31 divisions of a specific type of epidermal cell, called a gemma initial, which forms on the  
32 floor of the gemma cup [2, 3]. To investigate the regulatory mechanism underlying gemma  
33 development, we focused on two allelic mutants in which no gemma initial formed; these  
34 mutants were named *karappo*, meaning “empty”. We used whole-genome sequencing of  
35 both mutants, and molecular genetic analyses to identify the causal gene, *KARAPPO* (*KAR*),  
36 which encodes a Rop guanine nucleotide exchange factor (RopGEF) carrying a PRONE  
37 catalytic domain. *In vitro* GEF assays showed that the full-length KAR protein and the  
38 PRONE domain have significant GEF activity toward MpRop, the only Rop GTPase in *M.*  
39 *polymorpha*. Moreover, genetic complementation experiments showed a significant role for  
40 the N- and C-terminal variable regions in gemma development. Our investigation  
41 demonstrated an essential role for KAR/RopGEF in the initiation of plantlet development  
42 from a differentiated cell, which may involve cell polarity formation and subsequent  
43 asymmetric cell division via activation of Rop signaling, implying a similar developmental  
44 mechanism in vegetative reproduction of various land plants.

45

46 **KEYWORDS**

47 asexual reproduction, small GTPase, cell polarity, evolution

48

49 **RESULTS AND DISCUSSION**

50 **Gemma development in *Marchantia polymorpha***

51 Vegetative reproduction is a form of asexual reproduction in which clonal individuals  
52 develop directly from vegetative tissues, such as leaves, stems, and roots. Vegetative  
53 reproduction is a developmental process based on totipotency, which is the potential for a  
54 cell, even a differentiated cell, to regenerate organs or whole plantlets [4-6]. Many plants in  
55 diverse lineages exhibit vegetative reproduction, *e.g.* potato (*Solanum tuberosum*), which  
56 produces tubers in underground stems, *Kalanchoe diagremontiana*, which forms plantlets  
57 at the leaf margins, the Dhalia family, which develop root tubers, and the hen and chicken  
58 fern (*Asplenium bulbiferum*), which grows small bulbils on the top of fronds [7]. However,  
59 very little is known about the underlying molecular mechanisms of vegetative  
60 reproduction.

61 One of the most basal lineages in extant land plants, the liverwort *Marchantia*  
62 *polymorpha*, has the ability to propagate asexually by forming clonal plantlets, called  
63 gemmae, in a cupule or “gemma cup”, a cup-like receptacle formed on the dorsal side of  
64 the thallus, which is the gametophyte plant body (Figure S1A). The development of the  
65 gemma and gemma cup in *M. polymorpha* has been described on the basis of histological  
66 observations [2, 8]. In the basal floor of the gemma cup, epidermal cells undergo cell  
67 elongation followed by two cycles of asymmetrical cell division to form an apical gemma  
68 cell and a basal cell (Figure S1E). The gemma cell continues to divide and finally produces  
69 the discoid gemma with two laterally developed apical notches. The basal cell does not  
70 divide any further and differentiates into a stalk cell [1, 2]. Mucilage papillae also develop  
71 from individual epidermal cells located in the floor of gemma cups [2, 3]. In our  
72 histological observations, various stages of developing gemmae and single-celled mucilage

73 papillae (large club-shaped cells) were observed in the basal floor of the gemma cup  
74 (Figure S1B–D). The elongated morphology of mucilage papillae was distinct, with a  
75 number of single-membrane vesicles in their cytosol (Figure S1C). At the initial stage of  
76 gemma development, the basal stalk cell was already vacuolated, and the apical gemma cell  
77 underwent several rounds of periclinal cell divisions. In most cases, an anticlinal cell  
78 division was observed in the basal floor cell attached to the early stage of the developing  
79 gemma, while there was no cell division observed in the basal floor cell attached to the  
80 mucilage cell (Figure S1B–E).

81

## 82 **Isolation of *karappo-1* and *karappo-2* mutants**

83 In recent years, *M. polymorpha* has been exploited as a basal plant model system due to the  
84 availability of whole-genome sequence information, high-efficiency transformation  
85 methods, and genetic modification techniques [9-16].

86 To identify key regulator(s) involved in the initial stage of gemma development in  
87 *M. polymorpha*, we focused on two mutants, named *karappo-1* (*kar-1*) and *karappo-2*  
88 (*kar-2*), that show a common phenotype of impaired gemma formation. These two mutants  
89 were isolated independently; *kar-1* was isolated during the screening of T-DNA-tagged  
90 lines for morphological phenotypes of the gametophyte thallus [17], and *kar-2* was isolated  
91 from transgenic lines generated by biolistic delivery of a plasmid [18]. In the wild type as  
92 well as in *kar-1* and *kar-2* mutants, gemma cups formed at intervals on the dorsal side of  
93 thalli along the midrib (Figure 1A, B, and C). Numerous mature gemmae were observed  
94 from the top of the wild-type gemma cup; however, no gemmae were found in the *kar-1*  
95 and *kar-2* mutants (Figure 1F, G, and H). Transverse sections of the gemma cup showed no  
96 developing gemmae in the gemma-cup of the *kar-1* and *kar-2* mutants (Figure 1L, M, Q,

97 and R), while various stages of developing gemmae were observed in the wild type (Figure  
98 1K and P). In contrast, mucilage papillae were formed from the basal epidermis of the  
99 gemma cup in the *kar-1* and *kar-2* mutant as in the wild type (Figure 1U, V, and W). There  
100 was no distinct impairment in the other aspects of vegetative development in the *kar-1* and  
101 *kar-2* mutants compared to the wild type (*i.e.* growth rate of thalli, air chamber formation,  
102 and rhizoid development). These observations suggest that the initial stage of gemma  
103 development is defective in *kar-1* and *kar-2* mutants.

104

#### 105 **Molecular characterization of *kar* mutants**

106 The segregation ratio of the mutant gemma phenotype in an F<sub>1</sub> population generated from a  
107 cross between the *kar-1* mutant, which is a female, and the wild-type (WT) male accession  
108 Takaragaike-1 (Tak-1) was 102:108 (*kar*:WT). This fit the expected 1:1 ratio as indicated  
109 by the chi-squared test (p<0.01), suggesting the involvement of a single genetic locus in the  
110 *kar* phenotype. However, the *kar* phenotype in F<sub>1</sub> progenies segregated independently from  
111 the hygromycin-resistant marker in the transformed T-DNA fragment, indicating that the  
112 *kar-1* mutation is independent of the T-DNA insertion. The *kar-2* mutant, which is a male  
113 line, was infertile in several attempts at crossing with the wild-type female accession  
114 Takaragaike-2 (Tak-2).

115 To identify the causal gene of the *kar-1* and *kar-2* mutant phenotype, we  
116 sequenced the whole genomes of these mutants by next-generation DNA sequencing, and  
117 mapped the obtained reads on the reference genome of *M. polymorpha* [9]. Compared to  
118 the wild type, the *kar-1* mutant carried a 9-bp deletion and an 18-bp insertion at the  
119 junction of the 5th exon and 5th intron of *Mapoly0171s0028* [9]. As a result, the cDNA  
120 sequence of *Mapoly0171s0028* in the *kar1* mutant showed an 11-bp deletion and a 1-bp

121 insertion in the coding sequence, which caused a frame-shift and generated a truncated  
122 protein (Figure S2A–C). Furthermore, we identified a deletion of an approximately 20-kb  
123 genomic locus containing the entire coding sequence of *Mapoly0171s0028* in the *kar-2*  
124 mutant (Figure S2D and E).

125 We then performed genetic complementation tests in the *kar-1* and *kar-2* mutants  
126 by introducing the *Mapoly0171s0028* cDNA fragment under the control of its own  
127 promoter (*proKAR:KAR*). The resultant transgenic lines in the *kar-1* and *kar-2* mutant  
128 backgrounds had restored gemma formation (Figure 1I, J, N, O, S, and T). For further  
129 confirmation, we disrupted *Mapoly0171s0028* in the wild type using homologous  
130 recombination-mediated gene targeting [11] and isolated two independent knockouts of  
131 *Mapoly0171s0028* (Figure 2A and B). The two knockout lines, *kar<sup>KO</sup>* #1 and #2, showed a  
132 complete loss of gemma formation similar to the *kar* mutants. The impaired gemma  
133 formation was recovered by the introduction of citrine-fused wild-type cDNA of  
134 *Mapoly0171s0028* (Figure 2C–E). These results indicated that the *kar* phenotype was  
135 caused by a loss of function of *Mapoly0171s0028*. This gene was designated as *KARAPPO*  
136 (*KAR*) after a Japanese word meaning “empty”, representing the characteristic phenotype  
137 of the mutants with empty gemma cups.

138

### 139 ***KAR* encodes a potential activator of Rop GTPase signaling**

140 The deduced amino acid sequence of KAR encodes a highly conserved plant-specific Rop  
141 nucleotide exchanger (PRONE) catalytic domain, which is characteristic of the guanine  
142 nucleotide exchange factor (GEF) of the Rop GTPase [19], while the N- and C-terminal  
143 regions outside of the PRONE domain were highly variable (Figure S3). In angiosperms,  
144 Rop signaling mediated by RopGEF is involved in various developmental processes and

145 environmental responses [20-25]. *KAR* is the sole PRONE-type RopGEF gene in the *M.*  
146 *polymorpha* genome. In addition, the *M. polymorpha* genome also contains only a single  
147 copy of *Rop*, *Mapoly0051s0092*, designated as MpRop, which showed a high overall  
148 similarity to *Rop* in various plant lineages (Figure S4A and C).

149 To determine whether *KAR* encodes a functional GEF that acts on MpRop, we  
150 examined the interaction of KAR and MpRop by a yeast two-hybrid assay. Yeast cells  
151 co-transformed with a combination of either AD::KAR and BD::MpRop or AD::MpRop  
152 and BD::KAR grew on selective -W/L/H and -W/L/H/A medium (Figure 3A), indicating  
153 that KAR and MpRop physically interact. The interaction between KAR and MpRop was  
154 further confirmed by an *in vitro* pull-down assay. The predicted protein coding sequence of  
155 KAR was fused to the C-terminus of the 6x Histidine-tag. Purified 6xHis-KAR fusion  
156 proteins were pulled down with guanosine triphosphate (GTP)-bound, guanosine  
157 diphosphate (GDP)-bound, or nucleotide-free forms of the glutathione S-transferase  
158 (GST)-MpRop fusion protein and were detected using anti-His antibody. KAR fusion  
159 proteins exhibited similar interactions with different forms of MpRop *in vitro* (Figure 3B).

160 Next, we examined the GEF activity of KAR toward MpRop (Figure 3C). In  
161 *Arabidopsis thaliana*, there are 14 RopGEFs with a high degree of sequence similarity to  
162 the residues that are involved in catalyzing GDP/GTP exchange [26]. In Arabidopsis, the  
163 PRONE domain is sufficient for catalysis of nucleotide exchange on ROP [19] [26], while  
164 the variable C-terminal domain of some RopGEFs autoinhibits GEF activity [26]. To test  
165 the GEF activity and the potential regulatory role in the variable regions of KAR, we  
166 purified the full-length KAR protein and a truncated version of KAR containing just the  
167 PRONE domain (KAR-PRONE), and characterized their GEF activity toward MpRop  
168 using radio-labelled [<sup>35</sup>S]-GTP $\gamma$ S. We detected significant GEF activities toward MpRop

169 with full-length KAR and KAR-PRONE, and the GEF activity of full-length KAR was  
170 comparable to that of KAR-PRONE (Figure 3C).

171 We tested the functionality of the *KAR-PRONE* coding sequence without the N-  
172 and C-terminal region in gemma formation. Two lines with comparable expression levels  
173 of the full-length *KAR* or the *KAR-PRONE* coding sequence were selected for further  
174 analysis (Figure 3D). Introduction of citrine-fused full-length *KAR* cDNA restored to some  
175 extent the formation of gemma with normal morphology in the *kar*<sup>KO</sup> #2 background. By  
176 contrast, the citrine-fused KAR-PRONE did not lead to the full recovery of gemma  
177 formation; the most of the gemmae were abnormal in size and morphology with an  
178 irregular periphery (Figure 3E). These results demonstrated that the N-terminal and  
179 C-terminal variable regions of KAR play a significant role in proper gemma formation *in*  
180 *vivo*, although they have no obvious effect on GEF activity *in vitro* (Figure 3C).

181

## 182 **Ubiquitous expression of *KAR* and *MpRop* in vegetative tissues**

183 To evaluate the expression pattern of *KAR* and *MpRop*, we generated transgenic *M.*  
184 *polymorpha* lines expressing the β-glucuronidase (*GUS*) reporter gene under the control of  
185 the *KAR* promoter (*proKAR:GUS*) and the *MpRop* promoter (*proMpRop:GUS*). In  
186 *proKAR:GUS* and *proMpRop:GUS* lines, GUS staining was observed in the broader region  
187 of the entire thallus, including the basal floor of the gemma cups containing developing  
188 gemmae (Figure 4A and B). We further evaluated the expression pattern of *KAR* and  
189 *MpRop* using reverse-transcription quantitative PCR (RT-qPCR). Transcripts of *KAR* and  
190 *MpRop* were detected in all stages and organs in the vegetative thallus (Figure 4C). These  
191 results suggest that *KAR* and *MpRop* are ubiquitously and simultaneously expressed in the  
192 initial stage of gemma development.

193            Knockout plants of *MpRop* were generated by homologous  
194    recombination-mediated gene targeting; however, two independent *MpRop*<sup>KO</sup> lines showed  
195    severe impairment of thallus growth and wilted before the formation of the gemma cup  
196    (Figure S4B). This result suggests a much broader function for the sole Rop in *M.*  
197    *polymorpha*, which is evidently essential for the growth and development of the  
198    gametophyte thallus. Another type of GEF, SPIKE1 (SPK1), has been reported to regulate  
199    cytoskeletal rearrangement and cell-shape change in response to growth signals in  
200    angiosperms [27, 28]. SPK1 has a conserved DOCK homology region 2 (DHR2) domain,  
201    which is distantly related to CZH [CDM (Ced-5, Dock180, Myoblastcity)-Zizimin  
202    homology] RhoGEFs in animals and fungi [29]. *M. polymorpha* contains a single *SPK1*  
203    homologue, *MpSPK1* [9] (Figure S4C), which may have a critical function in controlling  
204    Rop signaling in thallus growth.

205            The contrast between the specific developmental impairment in *kar* mutant lines  
206    (Figure 1 and 2), and the ubiquitous promoter activity of *KAR* and *MpRop* (Figure 4),  
207    suggests an upstream regulatory mechanism for KAR activity, which enables cell-type  
208    specific activation of Rop in the gemma initial. Recent studies have shown that several  
209    plasma membrane-localized receptor-like protein kinases (RLKs) function as upstream  
210    regulators of Rop signaling through interaction with the C-terminal variable region of  
211    RopGEF (*i.e.* the pollen receptor kinases in tomato (*Solanum lycopersicum*) and FERONIA  
212    in *Arabidopsis thaliana*) [20, 21, 30]. Similar to their role in polarized cell growth mediated  
213    by Rop signaling in angiosperms, RLK(s) might be involved in the specific function of  
214    KAR in the initial stage of gemma development in *M. polymorpha*. Further functional  
215    studies on the N-terminal and C-terminal variable regions of KAR will be needed to  
216    understand the regulatory mechanism of Rop signaling in *M. polymorpha*.

217

218 **Role of KAR in the initial stage of gemma development**

219 In this study, we demonstrated that *KAR*, which encodes a RopGEF, is an essential factor  
220 required for the initial stage of gemma development in *M. polymorpha*. Histological studies  
221 have suggested the occurrence of cell protrusion and subsequent asymmetric cell divisions  
222 in the initial stage of gemma development in the epidermal floor of the gemma cup (Figure  
223 S1; [2]). A recent study in *M. polymorpha* demonstrated that a ROOT-HAIR DEFECTIVE  
224 SIX-LIKE (RSL) class I basic helix-loop-helix (bHLH) transcription factor, MpRSL1,  
225 controls the morphogenesis of structures derived from individual epidermal cells (*i.e.*  
226 rhizoids, slime papillae, mucilage papillae, and gemmae) [3]. Similar to the  
227 loss-of-function mutants of MpRSL1, in the *kar* mutants, we did not observe the one- or  
228 two-cell stage of gemma development. On the other hand, the other epidermis-derived  
229 structures, mucilage papillae and rhizoids, were generated normally in the *kar* mutants, but  
230 are absent in Mprsl1 mutants [3]. Mucilage papillae and rhizoids do not undergo any  
231 further cell division after polarized cell growth, whereas the development of gemmae  
232 involves subsequent asymmetrical cell division and further cell divisions. These  
233 observations suggest that KAR promotes the asymmetrical cell division(s) of the gemma  
234 precursor cell after the specification of an epidermal cell controlled by MpRSL1.

235 KAR contains a highly conserved PRONE domain (Figure S3), which has been  
236 implicated in the activity of the GEF of Rop GTPase [19, 26]. In this study, we  
237 demonstrated the GEF activity of KAR on MpRop *in vitro* (Figure 3). The *Arabidopsis*  
238 *thaliana* genome contains 14 RopGEFs, and Rop signaling mediated by RopGEF is  
239 involved in the control of polar cell growth of pollen tubes and root hairs [20-23]. This  
240 polar growth involves the coordination of cytoskeleton organization and vesicular

241 trafficking [31, 32]. In yeast and animals, the closest homologues of Rop, the Cdc42 Rho  
242 GTPases, regulate polarity and play a key role in the control of asymmetrical cell division  
243 [33, 34]. Recently in monocots, Rop was shown to be involved in the asymmetrical  
244 division of the stomata mother cell by controlling cytoskeletal scaffolds and nuclear  
245 positioning [35, 36]. KAR-mediated Rop signaling could function in the formation of cell  
246 polarity and/or subsequent asymmetrical cell divisions during the initiation of gemma  
247 development.

248 Vegetative reproduction can be considered as a type of naturally occurring somatic  
249 embryogenesis, in which a meristem is regenerated from differentiated cells. In the  
250 development of somatic embryos from single cells isolated from tissue cultures of carrot  
251 (*Daucus carota* subsp. *sativus*), the first cell division occurs asymmetrically, and one of the  
252 daughter cells gives rise to a three-dimensional cell mass from which one or more embryos  
253 develop [4-6]. Asymmetrical cell division to produce daughter cells of a different cell fate  
254 must be a common key process in the initial stage of organ/plantlet regeneration from  
255 differentiated cells. RopGEF-mediated Rop signaling seems to have been acquired in the  
256 common ancestor of land plants after the emergence of charophycean algae. PRONE-type  
257 RopGEFs have highly diverged in the course of land plant evolution, while the basal land  
258 plant *M. polymorpha* has a limited gene repertoire for Rop signaling (Figure S3 and S4).  
259 The Rop-driven asymmetric cell division of differentiated cells to regenerate clonal  
260 progenies could be a key innovation for sessile land plants to dominate the terrestrial  
261 ecosystem, and this mechanism may have been co-opted to regulate numerous  
262 physiological and developmental processes, probably also including vegetative  
263 reproduction or organ regeneration, in the course of land plant evolution.

264

265 **CONTACT FOR REAGENT AND RESOURCE SHARING**

266 Further information and requests for resources and reagents should be directed to and will  
267 be fulfilled by the Lead Contact, Kimitsune Ishizaki ([kimi@emerald.kobe-u.ac.jp](mailto:kimi@emerald.kobe-u.ac.jp)). Please  
268 note that the transfer of transgenic plants will be governed by an MTA, and will be  
269 dependent on appropriate import permits being acquired by the receiver.

270

271 **SUPPLEMENTAL INFORMATION**

272 Figures S1–S4, and Table S1.

273

274 **AUTHOR CONTRIBUTIONS**

275 T.H. and K.I. designed the research, and T.H. performed most of the experiments. K.I.  
276 isolated the *kar-1* mutant and H.K. performed linkage analyses. M.K. and K.T.Y. isolated  
277 *kar-2* mutants. T.H., Y.Y., and H.T. performed the histology. K.L.Q. and D.U. performed  
278 the *in vitro* pull-down and GEF assays. K.I., K.Y., S.Sh., S.Sa., and T.K. performed the  
279 whole-genome sequencing. M.S., M.W., and K.T. performed TEM analyses. T.H., K.I., and  
280 T.K. performed the gene-targeting experiments. T.H., K.I., Y.Y., D.U., H.F., and T.M.  
281 analyzed the data. T.H., Y.Y., and K.I. wrote the article.

282

283 **ACKNOWLEDGMENTS**

284 The authors thank Shohei Yamaoka and Ryuichi Nishihama for critically reading the  
285 manuscript; Tatsuaki Goh, Kohichi Toyokura, and Miwa Ohnishi for discussions; Sakiko  
286 Ishida, Yoriko Matsuda, and Chiho Hirata for technical assistance. Whole-genome  
287 sequencing was supported by NIBB Collaborative Research Programs (15-823 to K.I.).  
288 This study was supported by MEXT KAKENHI Grants-in-Aid for Scientific Research on  
289 Innovative Area (25113009 to T.K., and 25119711, 25114510, and 17H06472 to K.I.), JSPS  
290 KAKENHI Grants-in-Aid for Scientific Research (B) (15H04391 to K.I.), and by the Asahi  
291 Glass Foundation and SUNTORY Foundation for Life Sciences (to K.I.).

292

293 **FIGURE LEGENDS**

294 **Figure 1. Phenotype of the *kar* mutants and their complimented lines**

295 (A–Y) Five genotypes are presented, one in each column: (first column) wild type, (second  
296 column) *kar-1*, (third column) *kar-2*, (fourth column) *kar-1* complementation line (*kar-1*  
297 transformed with *proKAR:KAR*), (fifth column) *kar-2* complementation line (*kar-2*  
298 transformed with *proKAR:KAR*). (A–E) Top view of 2-week-old thalli grown from tips of  
299 thalli. Scale bars represent 1 mm. (F–J) Surface view of gemma cups in 2-week-old thalli.  
300 Scale bars represent 1 mm. (K–O) Toluidine-blue-stained transverse sections of gemma  
301 cups in 2-week-old plants. Scale bars represent 100  $\mu$ m. (P–Y) Magnified views of  
302 toluidine-blue-stained sections of gemma cups in 2-week-old plants. Arrowheads and  
303 arrows indicate gemma initials and mucilage papillae, respectively. Scale bars represent 10  
304  $\mu$ m.

305

306 **Figure 2. Generation of knockout mutants of *KAR***

307 (A) Schematic representation of the structure of the wild-type *KAR* locus (top), the  
308 construct designed for gene targeting (middle), and the *KAR* locus disrupted in the  
309 gene-targeted lines (bottom). Each primer pair used for genotyping is indicated by  
310 arrowheads and marked with (F) for forward or (R) for reverse. Open boxes indicate exons.  
311 (B) Genomic PCR analysis of the *KAR<sup>KO</sup>* lines using the primers indicated in (A). (C, D)  
312 Scanning electron microscopy of gemma cups in three genotypes are presented: *kar<sup>KO</sup>#1*  
313 (C), and a representative *kar<sup>KO</sup>* line transformed with *proKAR:C-KAR*, which contains a  
314 citrine-fused *KAR* coding sequence under the endogenous *KAR* promoter. (D). Scale bars  
315 represent 100  $\mu$ m. (E) Number of gemmae formed in a gemma cup in 3-week-old thalli  
316 grown from apical fragments in the wild type, a *kar<sup>KO</sup>* line, and a representative *kar<sup>KO</sup>*  
317 complemented line (Values are means  $\pm$  SD, n = 5).

318

319 **Figure 3. KAR has GEF activity towards MpRop.**

320 (A) Yeast two-hybrid experiments. Clones in the pGBKT7 vector containing the  
321 Gal4-binding domain (BD) are noted in the left column and clones in the pGADT7 vector  
322 containing the Gal4 activation domain (AD) are noted in the right column. Growth with

323 serial dilutions on the -L, -W dropout media indicates that both pGBKT7 and pGADT7  
324 vectors were present. Growth with serial dilutions on the -L, -W, -H dropout media and -L,  
325 -W, -H, -A dropout media indicates a physical interaction between the BD and AD fusion  
326 proteins. **(B)** Physical interaction of KAR with MpRop. His6-KAR was pulled down with  
327 GST or GST-MpRop1 using glutathione agarose. The pull-down samples were separated on  
328 a SDS-PAGE gel, then visualized by western blot with an anti-6xHis antibody. **(C)** GEF  
329 activity of the full-length KAR (KAR) or the PRONE domain of KAR (KAR-PRONE)  
330 toward MpRop. [<sup>35</sup>S]-GTP $\gamma$ S binding to 1  $\mu$ M GST-MpRop1 was analyzed over time at  
331 4°C. Graphs show data from two experiments. Fitting curves were estimated by the  
332 one-phase association model in GraphPad Prism software. **(D)** RT-qPCR analysis of *KAR*  
333 or *KAR-PRONE* expression in 3-week-old wild type and the respective complementation  
334 lines shown in Figure 3E. *MpAPT* was used as a control gene. Data are displayed as means  
335  $\pm$  SD ( $n = 3$ ). **(E)** Genetic complementation with the full-length *KAR* and the truncated  
336 *KAR* coding sequence containing only the PRONE domain. The histogram shows  
337 distribution of the different classes of gemmae in a gemma cup in 3-week-old thalli grown  
338 from apical fragments, in WT, a *kar*<sup>KO</sup> mutant, and two representative *kar* complementation  
339 lines with the full-length KAR (*proKAR:C-KAR*) and with the PRONE domain  
340 (*proKAR:C-PRONE*) (Values are means  $\pm$  s.d.,  $n=4\sim 5$ ). Tukey's test was performed for the  
341 number of normal gemmae, and letters above the bars indicate significant differences at  $p <$   
342 0.05. Right panels show pictures of normal gemma of over 500  $\mu$ m diameter (normal),  
343 abnormal gemma with more than two notches, and small gemma of less than 500  $\mu$ m  
344 diameter.  
345

#### 346 **Figure 4. Expression of KAR and MpRop in vegetative tissues**

347 **(A, B)** Histological GUS activity staining of representative proKAR:GUS **(A)** and  
348 proRop:GUS **(B)** transgenic lines. **(C)** RT-qPCR analysis of *KAR* and *MpRop* in  
349 1-week-old thalli yet to develop gemma cups (1w thallus), mature gemmae in gemma cups  
350 (gemma), gemma cups containing developing gemmae (gemma cups), and midribs. Total  
351 RNA was isolated from the respective tissues of Tak-1. *EF1 $\alpha$*  was used as a control gene.  
352 Data are displayed as means  $\pm$  SD ( $n = 3$ ).  
353

354 **STAR METHODS**

355

356 **KEY RESOURCES TABLE**

357

358 (Attached)

359

360 **CONTACT FOR REAGENT AND RESOURCE SHARING**

361 Further information and requests for resources and reagents should be directed to and will  
362 be fulfilled by the Lead Contact, Kimitsune Ishizaki ([kimi@emerald.kobe-u.ac.jp](mailto:kimi@emerald.kobe-u.ac.jp)). Please  
363 note that the transfer of transgenic lants will governed by an MTA, and will be dependent  
364 on appropriate import permits being acquired by the receiver.

365

366 **EXPERIMENTAL MODEL AND SUBJECT DETAILS**

367 **Plant Materials and Growth Conditions**

368 Female and male accessions of *M. polymorpha*, Takaragaike-2 (Tak-2) and Takaragaike-1  
369 [10], respectively (Ishizaki et al. 2008), were used as the wild type. F<sub>1</sub> spores generated by  
370 crossing Tak-2 and Tak-1 plants were used for transformation to generate the *kar-1* mutant  
371 and the *kar* knockout lines. Thalli were grown on 1% (w/v) agar medium containing  
372 half-strength Gamborg's B5 salts [37] under 50–60 μmol m<sup>-2</sup> s<sup>-1</sup> continuous white light  
373 with a cold cathode fluorescent lamp (CCFL; OPT-40C-N-L; Optrom, Japan) or white  
374 light-emitting diodes (white LED; VGL-1200W; SYNERGYTEC, Japan) at 22°C. For  
375 crossing, over 2-week-old thalli were transferred to continuous light conditions with 50–60  
376 μmol m<sup>-2</sup> s<sup>-1</sup> white LED and 20–30 μmol m<sup>-2</sup> s<sup>-1</sup> far red light-emitting diodes  
377 (VBL-TFL600-IR730, Valore, Japan).

378

379 **METHOD DETAILS**

380 **Phenotype Analysis and Histology**

381 Two-week-old thalli developed from tips of thalli were dissected into small pieces and  
382 transferred to fixative solution with 2% glutaraldehyde in 0.05 M phosphate buffer (pH 7.0)  
383 and evacuated with a water aspirator until the specimens sank, then fixed for 2 days at

384 room temperature. The samples were dehydrated in a graded ethanol series and embedded  
385 in Technovit 7100 plastic resin. Semi-thin sections (5- $\mu$ m thickness) were obtained with a  
386 microtome (HM 335E, Leica Microsystems) for light microscopy and stained with  
387 toluidine blue O. Sections were observed with an upright microscope (Axio Scope. A1,  
388 Carl Zeiss Microscopy).

389 Cultured thalli of *M. polymorpha* were observed using a digital microscope (VHX-5000,  
390 KEYENCE). For scanning electron microscopy, thalli were frozen in liquid nitrogen and  
391 observed with a scanning electron microscope (VHX-D500, KEYENCE).

392

### 393 **Electron microscopy**

394 Samples were fixed with 4% paraformaldehyde and 2% glutaraldehyde in 50 mM sodium  
395 cacodylate buffer (pH 7.4) for 2 h at room temperature and overnight at 4°C, then  
396 post-fixed with 1% osmium tetroxide in 50 mM cacodylate buffer for 3 h at room  
397 temperature. After dehydration in a graded methanol series (25, 50, 75, 90, and 100%), the  
398 samples were embedded in Epon812 resin (TAAB). Ultrathin sections (100 nm) or  
399 semi-thin sections (1  $\mu$ m) were cut by a diamond knife on an ultramicrotome (Leica EM  
400 UC7, Leica Microsystems, Germany) and placed on a glass slide. The sections were stained  
401 with 0.4% uranyl acetate followed by lead citrate solution and coated with osmium under  
402 an osmium coater (HPC-1SW, Vacuum Device, Japan). The coated sections were observed  
403 with a field-emission scanning electron microscope SU8220 (Hitachi High technology,  
404 Japan) with an yttrium aluminum garnet backscattered electron detector at an accelerating  
405 voltage of 5 kV.

406

### 407 **Genome sequencing of the *kar-1* and *kar-2* mutants**

408 Genomic DNA was extracted from *kar-1*, *kar-2*, and Tak-2 plants as follows: the tissue was  
409 powdered in liquid nitrogen and incubated in 10 mL hexadecyltrimethylammonium  
410 bromide (CTAB) buffer (1.5% CTAB, 75 mM Tris-HCl [pH 8.0], 15 mM EDTA, and 1 M  
411 NaCl) for 20 min at 56°C. This suspension was mixed with an equal volume of  
412 chloroform:isoamyl alcohol (24:1, w/v), incubated for 20 min at room temperature, and  
413 centrifuged at 4,000  $\times$  g for 20 min. The aqueous phase was used to repeat the

414 chloroform:isoamyl alcohol extraction, and then mixed gently with 1.5 volumes of CTAB  
415 precipitation buffer (1% CTAB, 50 mM Tris-HCl [pH 8.0], and 10 mM EDTA). After  
416 centrifugation at 10,000 × g for 30 min at 20°C, the precipitate was dissolved in 1 M  
417 sodium chloride containing 10 mg/mL RNaseA and incubated for 30 min at 37°C. The  
418 genomic DNA was precipitated with ethanol, dissolved in TE buffer (10 mM Tris-HCl [pH  
419 8.0] and 1 mM EDTA), and further purified using a Genomic-tip 100 column (QIAGEN,  
420 Germany). The DNA was then sheared on a Covaris sonicator (Covaris, USA),  
421 size-selected with Pippin Prep (Sage Science, USA), and used to create the libraries using  
422 the TruSeq DNA Sample Preparation Kit (Illumina) with an insert size of ~350 bp. The  
423 libraries were sequenced using Illumina HiSeq 2000 with a 2 × 101-nt paired-end  
424 sequencing protocol. The sequence reads were mapped to the *M. polymorpha* genome  
425 sequence [9] and the plasmid sequence was used for the biolistic transformation [18] by  
426 Bowtie2 v.2.2.9 [38] with default parameters, and visualized and assessed using Integrative  
427 Genomics Viewer v.2.3.23 [39].

428

#### 429 **Characterization of mutations in *KAR/Mapoly0171s0028***

430 Small pieces (3 × 3 mm) of thalli were taken from individual plants and crushed with a  
431 micro-pestle in 100 µl buffer containing 100 mM Tris-HCl, 1 M KCl, and 10 mM EDTA  
432 (pH 9.5). Sterilized water (400 µl) was added to each tube and a 1 µl aliquot of the extract  
433 was used as a template for PCR using KOD FX Neo DNA polymerase (Toyobo). To  
434 identify the mutation in the *kar-1* mutant, the *Mapoly0171s0028* locus was amplified by  
435 genomic PCR using the primer set kar-1\_gF/kar-1\_gR and sequenced. The cDNA of *kar* in  
436 the *kar-1* mutant was amplified by RT-PCR using the primer set KAR-cds-F/KAR-cds-sR  
437 and sequenced. To confirm the absence of *Mapoly0171s0028* in the *kar-2* mutant, genomic  
438 PCR was performed with a KOD FX Neo DNA polymerase using primers  
439 KAR-gF/KAR-gR. Primer pairs are shown in Figure S2D and Table S1.

440

#### 441 **Complementation tests**

442 For complementation of the *kar* mutants, the coding sequence of full-length *KAR* and the  
443 truncated coding sequence of *KAR* (*KAR-PRONE*), containing just the PRONE domain

444 (residues 132–503) were amplified by RT-PCR using KOD plus neo (TOYOBO) with the  
445 primer set KAR-cds-F/KAR-cds-sR and PRONE-L/PRONE-R, respectively. The *KAR* and  
446 *KAR-PRONE* coding sequence fragments were cloned into the pENTR/D-TOPO cloning  
447 vector (Life Technology) to produce pENTR-KAR and pENTR-PRONE, respectively. The  
448 *KAR* promoter region, including about 5 kb upstream of the initiation codon, was amplified  
449 from Tak-1 genomic DNA by PCR using KOD-Plus-Neo (TOYOBO) with the primer set  
450 KARpro\_GW\_F/KARpro\_GW\_302\_R. The PCR-amplified product was cloned into the  
451 *Xba*I and *Hind*III sites of pMpGWB302 to replace the CaMV35S promoter [40] with the  
452 In-Fusion HD cloning kit (Clontech, Mountain View, CA). The entry vector containing the  
453 *KAR* coding sequence was introduced into the binary vector by Gateway LR clonase II  
454 Enzyme mix (Thermo Fisher Scientific, USA) to generate the *proKAR:KAR* construct. The  
455 *proKAR:KAR* vector was introduced into regenerating thalli of *kar-1* and *kar-2* mutants via  
456 *Agrobacterium tumefaciens* GV2260 [13].

457 Similarly, the *KAR* promoter region, including about 5 kb upstream of the initiation codon,  
458 was amplified from Tak-1 genomic DNA by PCR using KOD-Plus-Neo (TOYOBO) with  
459 the primer set KARpro\_GW\_F/KARpro\_GW\_305\_R. The PCR-amplified product was  
460 cloned into the *Xba*I and *Hind*III sites of pMpGWB305, which contains citrine gene in  
461 front of the gateway cassette, to replace the CaMV35S promoter [40] with the In-Fusion  
462 HD cloning kit (Clontech, Mountain View, CA). The coding sequence fragments of *KAR*  
463 and *KAR-PRONE* in the entry vectors pENTR-KAR and pENTR-PRONE were introduced  
464 into the binary vectors by Gateway LR clonase II Enzyme mix (Thermo Fisher Scientific,  
465 USA) to generate the *proKAR:C-KAR*, and *proKAR:C-PRONE* constructs, respectively.  
466 The binary vector was transformed into the *kar*<sup>KO</sup> line. Transformants were selected with  
467 0.5 μM chlorsulfuron and 100 μg/ml cefotaxime.

468

#### 469 **Generation of *KAR*<sup>KO</sup> and *MpRop*<sup>KO</sup> plants**

470 To generate the *KAR*-targeting vector, 5'- and 3'-homologous arms (approximately 4.5-kb  
471 in length) were amplified from Tak-1 genomic DNA by PCR using KOD FX Neo  
472 (TOYOBO) with the primer pairs shown in Table S1. The PCR-amplified 5'- and  
473 3'-homologous arms were cloned into the *Pac*I and *Asc*I sites, respectively, of pJHY-TMp1

474 [11] with the In-Fusion HD cloning kit (Clontech, Mountain View, CA). The *KAR*-targeting  
475 vector was introduced into F<sub>1</sub> sporelings derived from sexual crosses between Tak-1 and  
476 Tak-2 via *Agrobacterium tumefaciens* GV2260 [10]. The transformed plants carrying the  
477 targeted insertions were selected by genomic PCR with a KOD FX Neo DNA polymerase  
478 and primer pairs shown in Figure 2 and Table S1.

479 To generate the *MpRop*-targeting vector, 5'- and 3'-homologous arms (approximately  
480 4.5-kb in length) were amplified from Tak-1 genomic DNA shown in Table S1. The  
481 PCR-amplified 5'- and 3 '-homologous arms were cloned into the *PacI* and *AscI* sites,  
482 respectively, of pJHY-TMp1 [11] with the In-Fusion HD cloning kit (Clontech, Mountain  
483 View, CA). The *MpRop*-targeting vector was transformed into F<sub>1</sub> sporelings derived from  
484 sexual crosses between Tak-1 and Tak-2 as described above. The transformed plants  
485 carrying the targeted insertions were selected by genomic PCR with a KOD FX Neo DNA  
486 polymerase and primer pairs shown in Figure S4B and Table S1.  
487

#### 488 **Promoter reporter analyses**

489 The *KAR* genomic sequence, including approximately 5 kb upstream of the initiation codon,  
490 was amplified from Tak-1 genomic DNA by PCR using KOD-Plus-Neo (TOYOBO) with  
491 the primer set KARpro\_F/KARpro\_R and was cloned into pENTR/D-TOPO (Thermo  
492 Fisher Scientific). Similarly, the *MpRop* genomic region, including about 3 kb upstream of  
493 the initiation codon, was amplified from Tak-1 genomic DNA by PCR with the primer set  
494 MpRoppro\_F/MpRoppro\_R and was inserted into pENTR/D-TOPO (Thermo Fisher).  
495 These entry vectors were introduced into the Gateway binary vector pMpGWB104 [40]  
496 using Gateway LR clonase II Enzyme mix (Thermo Fisher Scientific, USA) to generate  
497 *proKAR:GUS* and *proMpRop:GUS* binary constructs, respectively. The *proKAR:GUS* and  
498 *proMpRop:GUS* vectors were introduced into regenerating thalli of Tak-1 via  
499 *Agrobacterium tumefaciens* GV2260 [13]. Transformants were selected with 0.5 µM  
500 chlorsulfuron and 100 µg/ml cefotaxime. For histological GUS activity assays,  
501 transformants were incubated in GUS staining solution (0.5 mM potassium ferrocyanide,  
502 0.5 mM potassium ferricyanide, and 1 mM X-Gluc) at 37°C and later cleared with 70%  
503 ethanol (Jefferson et al., 1987).

504

505 **Yeast Two-Hybrid (Y2H) assay**

506 To construct AD::KAR and AD::MpRop vectors, the *KAR* and *MpRop* coding sequences  
507 were amplified by PCR using KOD plus neo (TOYOBO) with primer pairs  
508 *KAR\_WT\_Y2H\_pGADT7\_F* and *KAR\_WT\_Y2H\_pGADT7\_R*, and  
509 *Rop\_WT\_Y2H\_pGADT7\_F* and *Rop\_WT\_Y2H\_pGADT7\_R*, respectively, and subcloned  
510 into the *NotI* site of pGADT7-AD in Matchmaker Gold Yeast Two-Hybrid System (Takara  
511 Bio, Japan) with the In-Fusion HD cloning kit (Takara Bio). To construct BD::KAR and  
512 BD::MpRop vectors, the *KAR* and *MpRop* coding sequences were amplified by PCR using  
513 KOD plus neo (TOYOBO) with primer pairs *KAR\_WT\_Y2H\_pGBKT7\_F* and  
514 *KAR\_WT\_Y2H\_pGBKT7\_R*, and *Rop\_WT\_Y2H\_pGBKT7\_F* and  
515 *Rop\_WT\_Y2H\_pGBKT7\_R*, respectively, and subcloned into the *NotI* site of pGBKT7 in  
516 Matchmaker Gold Yeast Two-Hybrid System (Takara Bio) with the In-Fusion HD cloning  
517 kit (Takara Bio). Indicated combinations of plasmids were co-transformed into yeast strain  
518 Y2H Gold (Takara Bio) following the protocol for high-efficiency transformation of yeast  
519 with lithium acetate, single-stranded carrier DNA, and polyethylene glycol. Following  
520 transformation, colonies were selected for the presence of the plasmids, inoculated in liquid  
521 synthetic drop-out (SD) media (lacking the amino acids leucine and tryptophan, with the  
522 exception of untransformed strain Y2H Gold, which was grown in YPD), grown to  
523 saturation, and plated onto SD media plates lacking the indicated amino acids. SD media  
524 plates lacked the amino acids leucine, tryptophan, and histidine (SD -Leu/-Trp/-His).  
525 Serial 1:5 dilutions were made in water and 3 µl of each dilution was used to yield one spot.  
526 Plates were incubated at 30°C for two (SD -Leu/-Trp) or three (SD -Leu/-Trp/-His) days  
527 before taking pictures.

528

529 **Protein purification**

530 The cDNA of MpRop was amplified by RT-PCR using KOD plus neo (TOYOBO) with  
531 primer pairs MpRop-cds-F and MpRop-cds-sR and cloned into pENTR/D-TOPO (Thermo  
532 Fisher Scientific). The *MpRop* coding sequence in the resultant ENTRY clone and  
533 pENTR-KAR and pENTR-PRONE generated above were transferred using Gateway LR

534 clonase II Enzyme mix (Thermo Fisher Scientific, USA) into the bacterial expression  
535 vectors pDEST15 or pDEST17, which express GST- or 6xhistidine (6xHis)-tagged protein,  
536 respectively. 6xHis-KAR and 6xHis-KAR-PRONE were expressed in the *Escherichia coli*  
537 strain Arctic Express RP with 0.25 mM IPTG at 12°C. The cells were harvested by  
538 centrifugation and lysed in extraction buffer (20 mM Tris-HCl (pH 7.4), 200 mM NaCl, 2  
539 mM MgCl<sub>2</sub>, 5 mM 2-mercaptoethanol, 1 mM phenylmethane sulfonyl fluoride or  
540 phenylmethylsulfonyl fluoride (PMSF), 2 µg/ml leupeptin, 250 µg/ml lysozyme, and 0.2%  
541 C<sub>12</sub>E<sub>10</sub>) with sonication. The bacterial lysate was centrifuged at 100,000 x g for 1 hr.  
542 His-tagged protein was captured from the supernatant using nickel-NTA agarose, washed  
543 with wash buffer (20 mM Tris-HCl (pH 7.4), 500 mM NaCl, 5 mM 2-mercaptoethanol, 1  
544 mM PMSF, 2 µg/ml leupeptin, and 20 mM imidazole) and eluted with elution buffer (20  
545 mM Tris-HCl (pH 7.4), 150 mM NaCl, 5 mM 2-mercaptoethanol, 1 mM PMSF, and 20%  
546 glycerol) with 250 mM imidazole. The eluted proteins were dialyzed against elution buffer  
547 and frozen at -80°C.

548 Bacterial cells expressing GST or GST-MpRop were lysed in extraction buffer (50 mM  
549 Tris-HCl (pH 7.4), 150 mM NaCl, 2 mM MgCl<sub>2</sub>, 1 mM EDTA, 5 mM 2-mercaptoethanol,  
550 1 mM PMSF, 2 µg/ml leupeptin, 100 µM GDP, 250 µg/ml lysozyme, and 0.2% C<sub>12</sub>E<sub>10</sub>)  
551 with sonication. The bacterial lysate was centrifuged at 100,000 x g for 1 hr. GST-tagged  
552 proteins were captured from the supernatant using glutathione-agarose, washed with wash  
553 buffer I (50 mM Tris-HCl (pH 7.4), 100 mM NaCl, 1 mM EDTA, 5 mM 2-mercaptoethanol,  
554 40 µM GDP, 2 mM MgCl<sub>2</sub>, 1 mM PMSF, and 2 µg/ml leupeptin), wash Buffer II (50 mM  
555 Tris-HCl (pH 7.4), 500 mM NaCl, 40 µM GDP, 2 mM MgCl<sub>2</sub>, 1 mM EDTA, 5 mM  
556 2-mercaptoethanol, 1 mM PMSF, and 2 µg/ml leupeptin), then wash buffer I again.  
557 GST-tagged proteins were eluted with elution buffer (100 mM Tris-HCl (pH 8.8), 200 mM  
558 NaCl, 40 µM GDP, 2 mM MgCl<sub>2</sub>, 10 mM 2-mercaptoethanol, 1 mM EDTA, 1 mM PMSF,  
559 and 20% glycerol) with 20 mM glutathione. The eluted proteins were dialyzed against  
560 elution buffer without GDP and frozen at -80°C.

561

## 562 ***In vitro* pull-down assay**

563 One µg of 6xHis-KAR was incubated with 10 µg of GST or GST-MpROP in Nucleotide

564 Binding Buffer (20 mM HEPES-NaOH (pH 7.4), 5 mM MgCl<sub>2</sub>, 1 mM dithiothreitol, 0.1%  
565 Triton X-100, and 1 mM EDTA) preloaded with 10 µM GDP, GTPγS, or no nucleotide for  
566 4 hours at 4°C. The samples were centrifuged with a table-top centrifuge at full speed for 1  
567 min, and the supernatant was incubated with Glutathione-agarose resin for 30 min at 4°C.  
568 The resins were then washed for three times with Nucleotide Binding Buffer with the  
569 respective nucleotide. The resins were then boiled with SDS loading buffer and separated  
570 by sodium dodecyl sulfate polyacrylamide gel electrophoresis (SDS-PAGE). The  
571 6xHis-tagged proteins were detected by western blot with a mouse anti-6xHis antibody  
572 (Santa Cruz Biotech) as the primary antibody, an HRP-conjugated anti-mouse IgG antibody  
573 was used as the secondary antibody. GST and GST-MpRop were detected by Coomassie  
574 Brilliant Blue staining.

575

### 576 **GTPγS binding on MpRop**

577 The GEF enzymatic activity of KAR or KAR-PRONE toward MpRop was analyzed using  
578 radio-labelled [<sup>35</sup>S]-GTPγS, as described in previous studies with slight modifications [26,  
579 41]. For [<sup>35</sup>S]-GTPγS binding, 2 µM GST-MpRop in reaction buffer (50 mM Tris-HCl (pH  
580 7.4), 1 mM EDTA, 1 mM DTT, and 5 mM MgCl<sub>2</sub>) was mixed with an equal volume of  
581 reaction buffer containing 5 µM [<sup>35</sup>S]-GTPγS to start the exchange reaction on ice. At given  
582 time points, 50 µl aliquots were removed and placed into 450 µl of ice-cold wash buffer  
583 (20 mM Tris-HCl (pH 7.4), 100 mM NaCl, and 25 mM MgCl<sub>2</sub>) with 0.1 mM GTP, then  
584 applied to a nitrocellulose membrane filter. The filter was washed three times with 2 to 3  
585 ml of ice-cold wash buffer. The amount of [<sup>35</sup>S]-GTPγS was measured by scintillation  
586 counting.

587

### 588 **RT-qPCR**

589 Total RNA was isolated from the 1-week-old thalli, and mature gemmae, gemma cups, and  
590 midribs of 3-week-old thalli of Tak-1 (Fig. 4C) and 1-week-old thalli of the *kar*<sup>KO</sup>#2 line  
591 transformed with *proKAR:Citrine-KAR* or *proKAR:Citrine-PRONE* (Fig. 3D) using the  
592 RNeasy Plant mini kit (Qiagen). One µg of total RNA was reverse-transcribed in a 20 µl  
593 reaction mixture using ReverTra Ace qPCR RT Master Mix with gDNA remover

594 (TOYOBO). After the reaction, the mixture was diluted with 40 µl of distilled water and 2  
595 µl aliquots were used for quantitative PCR (qPCR) analysis. qPCR was performed with the  
596 Light Cycler 96 (Roche) using KOD SYBR qRT-PCR Mix (TOYOBO) according to the  
597 manufacturer's protocol. The primers used in these experiments are listed in Table S1.  
598 Transcript levels of MpEF1a or MpAPT were used as a reference for normalization [42].  
599 RT-qPCR experiments were performed using three biological replicates and technically  
600 duplicated.

601

## 602 Phylogenetic Analysis of KAR

603 For phylogenetic analysis of KAR and RopGEFs, peptide sequences were collected from  
604 genomic information of *M. polymorpha* in MalpolBase (<http://marchantia.info/>), *A.*  
605 *thaliana* in TAIR (<http://www.arabidopsis.org>), *Physcomitrella patens* [43] and *Selaginella*  
606 *moellendorffii* [44] in Phytozome (<https://phytozome.jgi.doe.gov/pv/portal.html>), and  
607 *Klebsormidium nitens* NIES-2285 in  
608 ([http://www.plantmorphogenesis.bio.titech.ac.jp/~algaе\\_genome\\_project/klebsormidium/kf\\_download.htm](http://www.plantmorphogenesis.bio.titech.ac.jp/~algaе_genome_project/klebsormidium/kf_download.htm)) [45]. A multiple alignment of amino acid sequences of KAR and its  
609 homologous RopGEFs was first constructed using the MUSCLE program [46]  
610 implemented in MEGA6.06 [47] with default parameters, which was performed using a  
611 Maximum Likelihood method by PhyML [48] with the LG+G+I substitution model. One  
612 thousand bootstrap replicates were performed in each analysis to obtain the confidence  
613 support.

615

616 REFERENCES

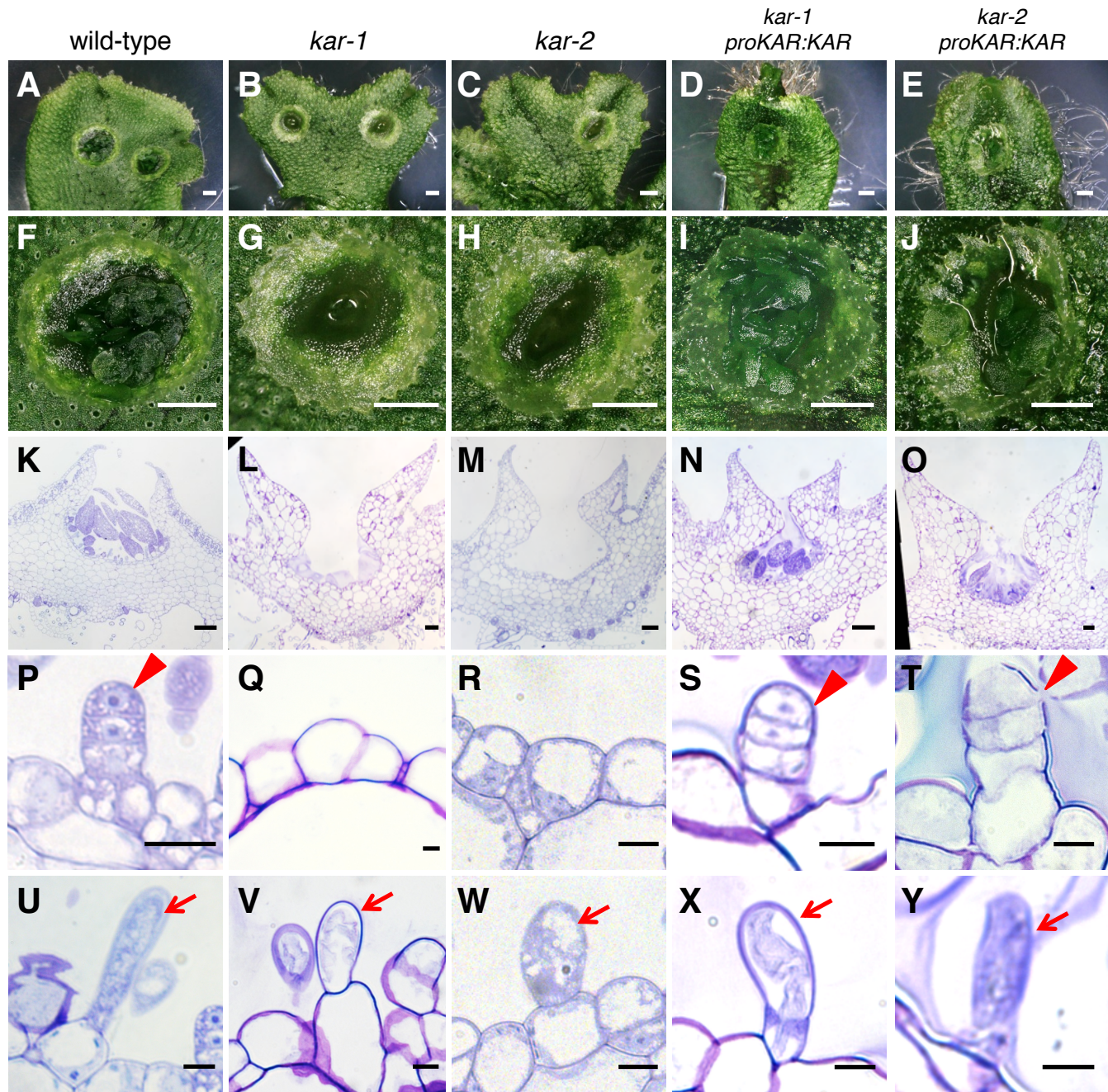
- 617 1. Shimamura, M. (2016). *Marchantia polymorpha*: Taxonomy, phylogeny and  
618 morphology of a model system. *Plant Cell Physiol.* *57*, 230-256.
- 619 2. Barnes, C.R., and Land, W.J.G. (1908). Bryological papers. II. The origin of the  
620 cupule of Marchantia. *Bot. Gaz.* *46*, 401-409.
- 621 3. Proust, H., Honkanen, S., Jones, Victor A.S., Morieri, G., Prescott, H., Kelly, S.,  
622 Ishizaki, K., Kohchi, T., and Dolan, L. (2016). RSL class I genes controlled the  
623 development of epidermal structures in the common ancestor of land plants. *Curr.  
624 Biol.* *26*, 93-99.
- 625 4. Steward, F.C., Mapes, M.O., and Mears, K. (1958). Growth and organized  
626 development of cultured cells. II. Organization in cultures grown from freely  
627 suspended cells. *Am. J. Bot.* *45*, 705-708.
- 628 5. Steward, F.C., Mapes, M.O., Kent, A.E., and Holsten, R.D. (1964). Growth and  
629 development of cultured plant cells. *Science* *143*, 20-27.
- 630 6. Steeves, T.A., and Sussex, I.M. (1989). Patterns in plant development, 2 Edition,  
631 (Cambridge: Cambridge University Press).
- 632 7. Davis, F.T., Geneve, R.L., Wilson, S.E., Hartmann, H.T., Kester, D.E. (2017).  
633 Hartmann & Kester's Plant Propagation: Principles and Practices, (Pearson).
- 634 8. Hofmeister, W.F.B. (1862). On the germination, development, and fructification of  
635 the higher Cryptogamia, and on the fructification of the Coniferae., (London, Pub.  
636 for the Ray society).
- 637 9. Bowman, J.L., Kohchi, T., Yamato, K.T., Jenkins, J., Shu, S., Ishizaki, K., Yamaoka,  
638 S., Nishihama, R., Nakamura, Y., Berger, F., et al. (2017). Insights into land plant  
639 evolution garnered from the *Marchantia polymorpha* genome. *Cell* *171*, 287-304  
640 e215.
- 641 10. Ishizaki, K., Chiyoda, S., Yamato, K.T., and Kohchi, T. (2008).  
642 *Agrobacterium*-mediated transformation of the haploid liverwort *Marchantia*  
643 *polymorpha* L., an emerging model for plant biology. *Plant Cell Physiol.* *49*,  
644 1084-1091.
- 645 11. Ishizaki, K., Johzuka-Hisatomi, Y., Ishida, S., Iida, S., and Kohchi, T. (2013).  
646 Homologous recombination-mediated gene targeting in the liverwort *Marchantia*  
647 *polymorpha* L. *Sci. Rep.* *3*, 1532.
- 648 12. Ishizaki, K., Nishihama, R., Yamato, K.T., and Kohchi, T. (2016). Molecular  
649 genetic tools and techniques for *Marchantia polymorpha* research. *Plant Cell  
650 Physiol.* *57*, 262-270.
- 651 13. Kubota, A., Ishizaki, K., Hosaka, M., and Kohchi, T. (2013). Efficient

- 652                  Agrobacterium-mediated transformation of the liverwort *Marchantia polymorpha*  
653                  using regenerating thalli. Biosci. Biotechnol. Biochem. 77, 167-172.
- 654    14. Sugano, S.S., Shirakawa, M., Takagi, J., Matsuda, Y., Shimada, T., Hara-Nishimura,  
655                  I., and Kohchi, T. (2014). CRISPR/Cas9-mediated targeted mutagenesis in the  
656                  liverwort *Marchantia polymorpha* L. Plant Cell Physiol. 55, 475-481.
- 657    15. Nishihama, R., Ishida, S., Urawa, H., Kamei, Y., and Kohchi, T. (2016). Conditional  
658                  gene expression/deletion systems for *Marchantia polymorpha* using its own  
659                  heat-shock promoter and Cre/loxP-mediated site-specific recombination. Plant Cell  
660                  Physiol. 57, 271-280.
- 661    16. Flores-Sandoval, E., Dierschke, T., Fisher, T.J., and Bowman, J.L. (2016). Efficient  
662                  and inducible use of artificial microRNAs in *Marchantia polymorpha*. Plant Cell  
663                  Physiol. 57, 281-290.
- 664    17. Ishizaki, K., Mizutani, M., Shimamura, M., Masuda, A., Nishihama, R., and Kohchi,  
665                  T. (2013). Essential role of the E3 ubiquitin ligase NOPPERABO1 in schizogenous  
666                  intercellular space formation in the liverwort *Marchantia polymorpha*. Plant Cell 25,  
667                  4075-4084.
- 668    18. Takenaka, M., Yamaoka, S., Hanajiri, T., Shimizu-Ueda, Y., Yamato, K.T.,  
669                  Fukuzawa, H., and Ohyama, K. (2000). Direct transformation and plant  
670                  regeneration of the haploid liverwort *Marchantia polymorpha* L. Transgenic Res. 9,  
671                  179-185.
- 672    19. Berken, A., Thomas, C., and Wittinghofer, A. (2005). A new family of RhoGEFs  
673                  activates the Rop molecular switch in plants. Nature 436, 1176-1180.
- 674    20. Zhang, Y., and McCormick, S. (2007). A distinct mechanism regulating a  
675                  pollen-specific guanine nucleotide exchange factor for the small GTPase Rop in  
676                  *Arabidopsis thaliana*. Proc. Natl. Acad. Sci. U. S. A. 104, 18830-18835.
- 677    21. Duan, Q., Kita, D., Li, C., Cheung, A.Y., and Wu, H.M. (2010). FERONIA  
678                  receptor-like kinase regulates RHO GTPase signaling of root hair development.  
679                  Proc. Natl. Acad. Sci. U. S. A. 107, 17821-17826.
- 680    22. Kessler, S.A., Shimosato-Asano, H., Keinath, N.F., Wuest, S.E., Ingram, G.,  
681                  Panstruga, R., and Grossniklaus, U. (2010). Conserved molecular components for  
682                  pollen tube reception and fungal invasion. Science 330, 968-971.
- 683    23. Nibau, C., and Cheung, A.Y. (2011). New insights into the functional roles of  
684                  CrRLKs in the control of plant cell growth and development. Plant signaling &  
685                  behavior 6, 655-659.
- 686    24. Oda, Y., and Fukuda, H. (2012). Initiation of cell wall pattern by a Rho- and  
687                  microtubule-driven symmetry breaking. Science 337, 1333-1336.
- 688    25. Li, Z., Waadt, R., and Schroeder, J.I. (2016). Release of GTP exchange factor

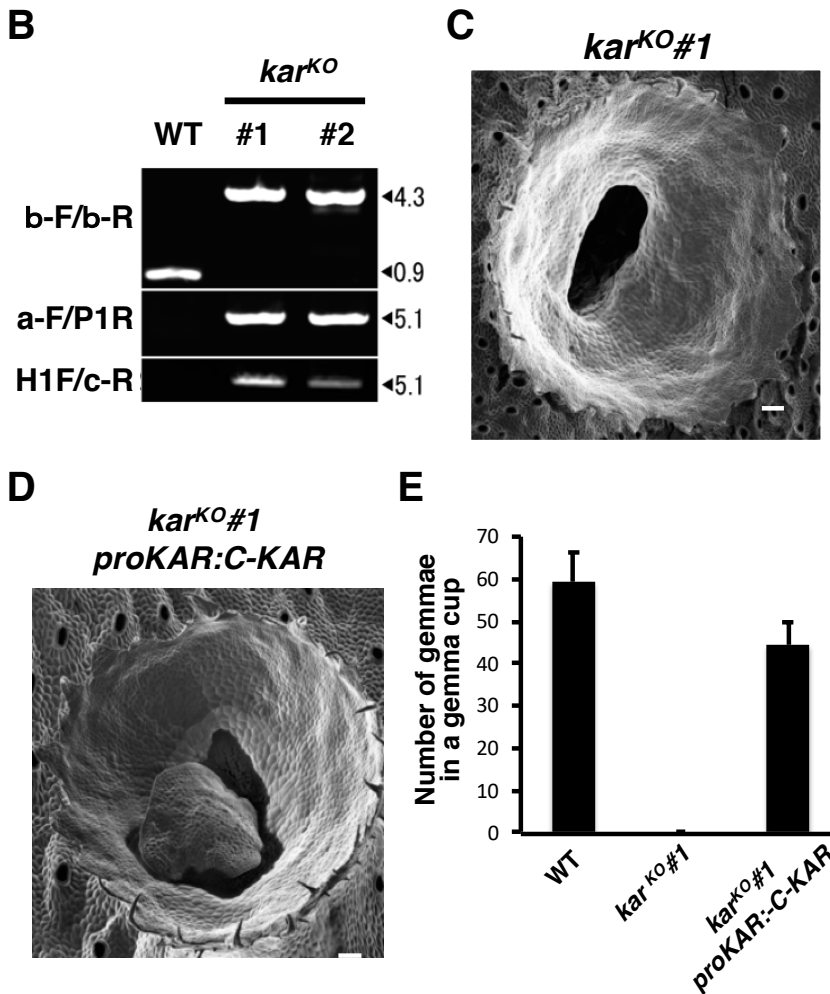
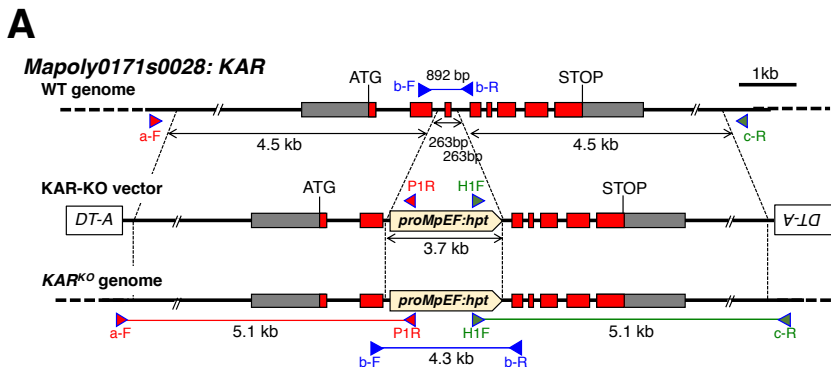
- 689                   mediated down-regulation of abscisic acid signal transduction through  
690                   ABA-Induced rapid degradation of RopGEFs. *PLoS Biol.* *14*, e1002461.
- 691     26. Gu, Y., Li, S., Lord, E.M., and Yang, Z. (2006). Members of a novel class of  
692                   Arabidopsis Rho guanine nucleotide exchange factors control Rho  
693                   GTPase-dependent polar growth. *Plant Cell* *18*, 366-381.
- 694     27. Basu, D., Le, J., Zakharova, T., Mallory, E.L., and Szymanski, D.B. (2008). A  
695                   SPIKE1 signaling complex controls actin-dependent cell morphogenesis through  
696                   the heteromeric WAVE and ARP2/3 complexes. *Proc. Natl. Acad. Sci. U. S. A.* *105*,  
697                   4044-4049.
- 698     28. Zhang, C., Kotchoni, S.O., Samuels, A.L., and Szymanski, D.B. (2010). SPIKE1  
699                   signals originate from and assemble specialized domains of the endoplasmic  
700                   reticulum. *Curr. Biol.* *20*, 2144-2149.
- 701     29. Meller, N., Merlot, S., and Guda, C. (2005). CZH proteins: a new family of  
702                   Rho-GEFs. *J. Cell Sci.* *118*, 4937-4946.
- 703     30. Chang, F., Gu, Y., Ma, H., and Yang, Z. (2013). AtPRK2 promotes ROP1 activation  
704                   via RopGEFs in the control of polarized pollen tube growth. *Molecular plant* *6*,  
705                   1187-1201.
- 706     31. Fu, Y., Gu, Y., Zheng, Z., Wasteneys, G., and Yang, Z. (2005). *Arabidopsis*  
707                   interdigitating cell growth requires two antagonistic pathways with opposing action  
708                   on cell morphogenesis. *Cell* *120*, 687-700.
- 709     32. Gu, Y., Fu, Y., Dowd, P., Li, S., Vernoud, V., Gilroy, S., and Yang, Z. (2005). A Rho  
710                   family GTPase controls actin dynamics and tip growth via two counteracting  
711                   downstream pathways in pollen tubes. *J. Cell Biol.* *169*, 127-138.
- 712     33. Etienne-Manneville, S. (2004). Cdc42--the centre of polarity. *J. Cell Sci.* *117*,  
713                   1291-1300.
- 714     34. Park, H.O., and Bi, E. (2007). Central roles of small GTPases in the development of  
715                   cell polarity in yeast and beyond. *Microbiol. Mol. Biol. Rev.* *71*, 48-96.
- 716     35. Humphries, J.A., Vejrupkova, Z., Luo, A., Meeley, R.B., Sylvester, A.W., Fowler,  
717                   J.E., and Smith, L.G. (2011). ROP GTPases act with the receptor-like protein PAN1  
718                   to polarize asymmetric cell division in maize. *Plant Cell* *23*, 2273-2284.
- 719     36. Facette, M.R., Park, Y., Sutimananapi, D., Luo, A., Cartwright, H.N., Yang, B.,  
720                   Bennett, E.J., Sylvester, A.W., and Smith, L.G. (2015). The SCAR/WAVE complex  
721                   polarizes PAN receptors and promotes division asymmetry in maize. *Nature Plants*  
722                   *1*, 14024.
- 723     37. Gamborg, O.L., Miller, R.A., and Ojima, K. (1968). Nutrient requirements of  
724                   suspension cultures of soybean root cells. *Exp. Cell Res.* *50*, 151-158.
- 725     38. Langmead, B., and Salzberg, S.L. (2012). Fast gapped-read alignment with Bowtie

- 726            2. Nat. Methods 9.
- 727    39. Robinson, J.T., Thorvaldsdottir, H., Winckler, W., Guttman, M., Lander, E.S., Getz,  
728            G., and Mesirov, J.P. (2011). Integrative genomics viewer. Nat. Biotechnol. 29,  
729            24-26.
- 730    40. Ishizaki, K., Nishihama, R., Ueda, M., Inoue, K., Ishida, S., Nishimura, Y., Shikanai,  
731            T., and Kohchi, T. (2015). Development of Gateway binary vector series with four  
732            different selection markers for the liverwort *Marchantia polymorpha*. PLoS One 10,  
733            e0138876.
- 734    41. Urano, D., Jones, J.C., Wang, H., Matthews, M., Bradford, W., Bennetzen, J.L., and  
735            Jones, A.M. (2012). G protein activation without a GEF in the plant kingdom. PLoS  
736            Genet. 8, e1002756.
- 737    42. Saint-Marcoux, D., Proust, H., Dolan, L., and Langdale, J.A. (2015). Identification  
738            of Reference Genes for Real-Time Quantitative PCR Experiments in the Liverwort  
739            *Marchantia polymorpha*. PLoS One 10, e0118678.
- 740    43. Rensing, S.A., Lang, D., Zimmer, A.D., Terry, A., Salamov, A., Shapiro, H.,  
741            Nishiyama, T., Perroud, P.F., Lindquist, E.A., Kamisugi, Y., et al. (2008). The  
742            Physcomitrella genome reveals evolutionary insights into the conquest of land by  
743            plants. Science 319, 64-69.
- 744    44. Banks, J.A., Nishiyama, T., Hasebe, M., Bowman, J.L., Grabskov, M., dePamphilis,  
745            C., Albert, V.A., Aono, N., Aoyama, T., Ambrose, B.A., et al. (2011). The  
746            Selaginella genome identifies genetic changes associated with the evolution of  
747            vascular plants. Science 332, 960-963.
- 748    45. Hori, K., Maruyama, F., Fujisawa, T., Togashi, T., Yamamoto, N., Seo, M., Sato, S.,  
749            Yamada, T., Mori, H., Tajima, N., et al. (2014). *Klebsormidium flaccidum* genome  
750            reveals primary factors for plant terrestrial adaptation. Nat Commun 5, 3978.
- 751    46. Edgar, R.C. (2004). MUSCLE: multiple sequence alignment with high accuracy  
752            and high throughput. Nucleic Acids Res. 32, 1792-1797.
- 753    47. Tamura, K., Stecher, G., Peterson, D., Filipski, A., and Kumar, S. (2013). MEGA6:  
754            Molecular Evolutionary Genetics Analysis version 6.0. Mol. Biol. Evol. 30,  
755            2725-2729.
- 756    48. Guindon, S., Dufayard, J.F., Lefort, V., Anisimova, M., Hordijk, W., and Gascuel, O.  
757            (2010). New algorithms and methods to estimate maximum-likelihood phylogenies:  
758            assessing the performance of PhyML 3.0. Syst. Biol. 59, 307-321.
- 759

Figure1-4

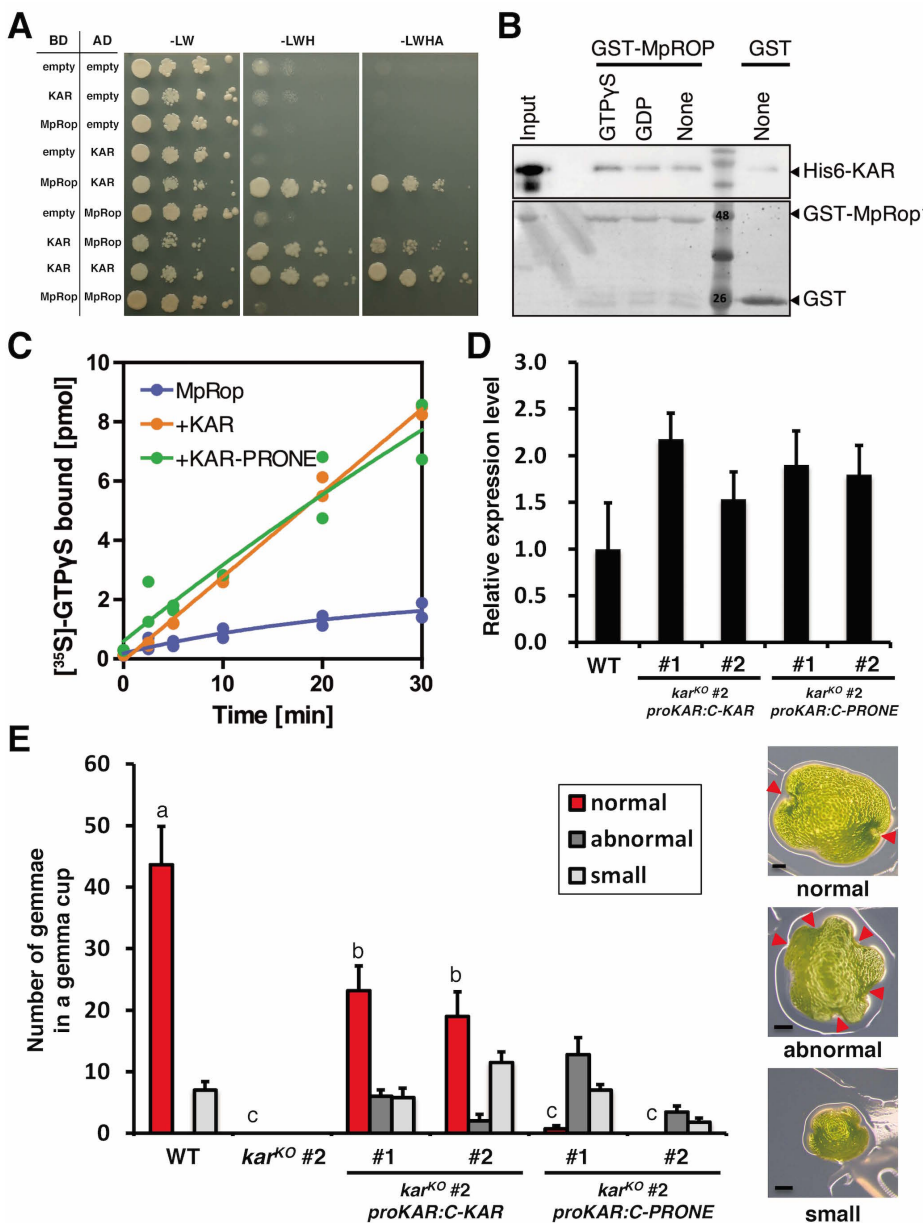
**Figure 1. Phenotype of the *kar* mutants and their complimented lines**

(A–Y) Five genotypes are presented, one in each column: (first column) wild type, (second column) *kar-1*, (third column) *kar-2*, (fourth column) *kar-1* complementation line (*kar-1* transformed with *proKAR:KAR*), (fifth column) *kar-2* complementation line (*kar-2* transformed with *proKAR:KAR*). (A–E) Top view of 2-week-old thalli grown from tips of thalli. Scale bars represent 1 mm. (F–J) Surface view of gemma cups in 2-week-old thalli. Scale bars represent 1 mm. (K–O) Toluidine-blue-stained transverse sections of gemma cups in 2-week-old plants. Scale bars represent 100  $\mu$ m. (P–Y) Magnified views of toluidine-blue-stained sections of gemma cups in 2-week-old plants. Arrowheads and arrows indicate gemma initials and mucilage papillae, respectively. Scale bars represent 10  $\mu$ m.



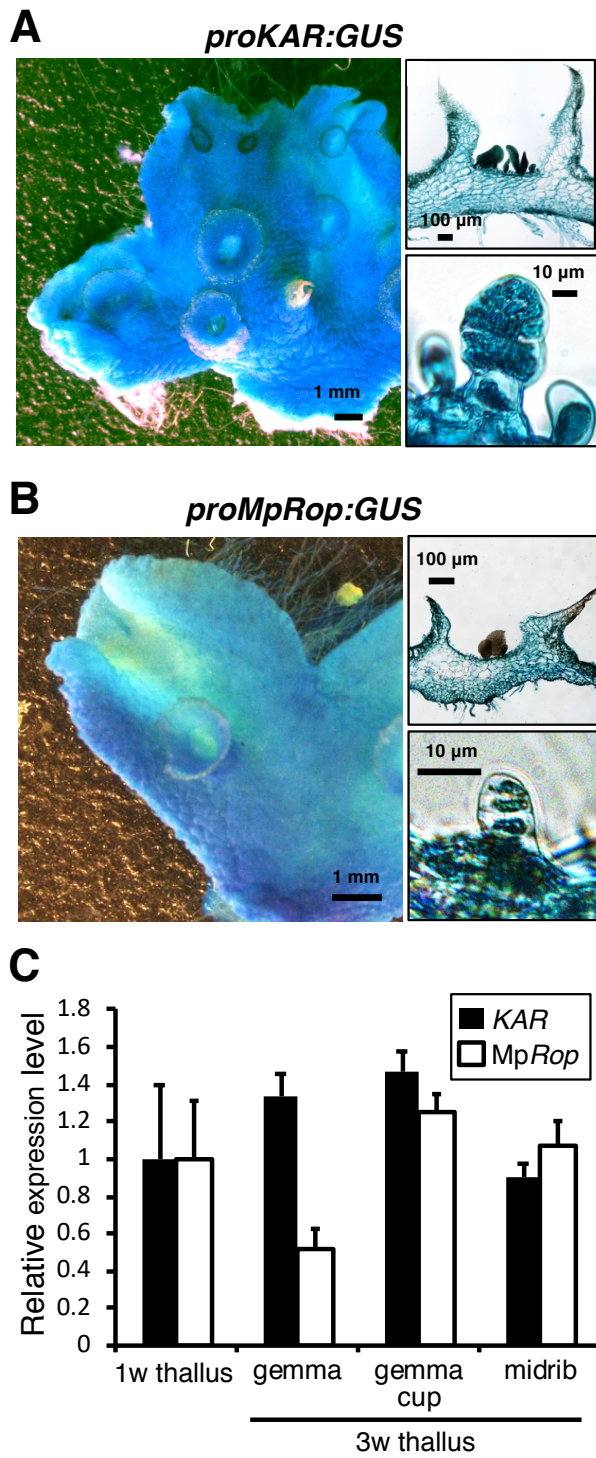
**Figure 2. Generation of knockout mutants of *KAR***

(A) Schematic representation of the structure of the wild-type *KAR* locus (top), the construct designed for gene targeting (middle), and the *KAR* locus disrupted in the gene-targeted lines (bottom). Each primer pair used for genotyping is indicated by arrowheads and marked with (F) for forward or (R) for reverse. Open boxes indicate exons. (B) Genomic PCR analysis of the *KAR<sup>KO</sup>* lines using the primers indicated in (A). (C, D) Scanning electron microscopy of gemma cups in three genotypes are presented: *kar<sup>KO</sup>#1* (C), and a representative *kar<sup>KO</sup>* line transformed with *proKAR:C-KAR*, which contains a citrine-fused *KAR* coding sequence under the endogenous *KAR* promoter. (D). Scale bars represent 100  $\mu$ m. (E) Number of gemmae formed in a gemma cup in 3-week-old thalli grown from apical fragments in the wild type, a *kar<sup>KO</sup>* line, and a representative *kar<sup>KO</sup>* complemented line (Values are means  $\pm$  SD, n = 5).



**Figure 3. KAR has GEF activity towards MpRop.**

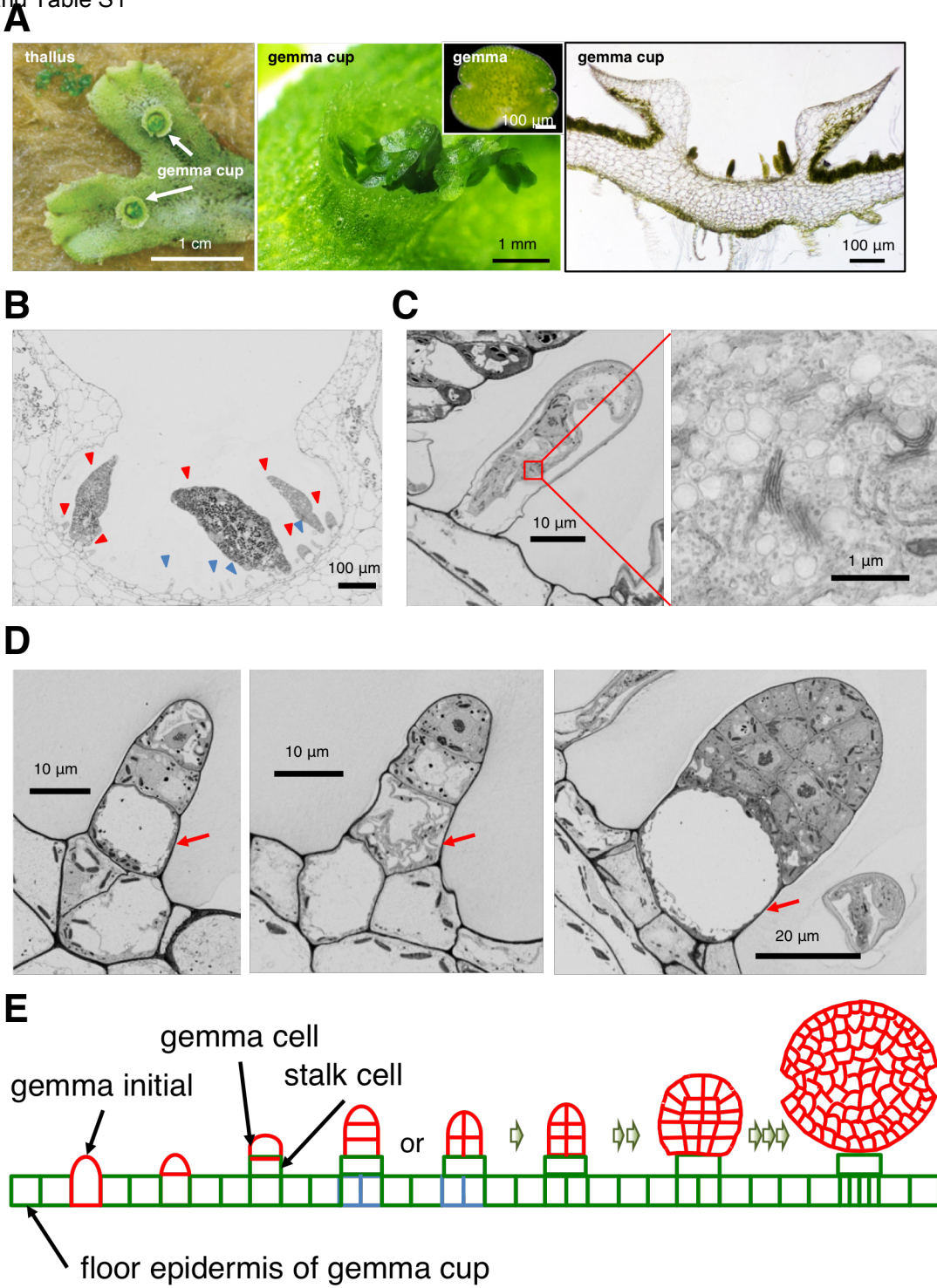
**(A)** Yeast two-hybrid experiments. Clones in the pGBKT7 vector containing the Gal4-binding domain (BD) are noted in the left column and clones in the pGADT7 vector containing the Gal4 activation domain (AD) are noted in the right column. Growth with serial dilutions on the -L, -W dropout media indicates that both pGBKT7 and pGADT7 vectors were present. Growth with serial dilutions on the -L, -W, -H dropout media and -L, -W, -H, -A dropout media indicates a physical interaction between the BD and AD fusion proteins. **(B)** Physical interaction of KAR with MpRop. His6-KAR was pulled down with GST or GST-MpRop1 using glutathione agarose. The pull-down samples were separated on a SDS-PAGE gel, then visualized by western blot with an anti-6xHis antibody. **(C)** GEF activity of the full-length KAR (KAR) or the PRONE domain of KAR (KAR-PRONE) toward MpRop. [ $^{35}$ S]-GTP $\gamma$ S binding to 1  $\mu$ M GST-MpRop1 was analyzed over time at 4° C. Graphs show data from two experiments. Fitting curves were estimated by the one-phase association model in GraphPad Prism software. **(D)** RT-qPCR analysis of *KAR* or *KAR-PRONE* expression in 3-week-old wild type and the respective complementation lines shown in Figure 3E. MpAPT was used as a control gene. Data are displayed as means  $\pm$  SD ( $n = 3$ ). **(E)** Genetic complementation with the full-length *KAR* and the truncated *KAR* coding sequence containing only the PRONE domain. The histogram shows distribution of the different classes of gemmae in a gemma cup in 3-week-old thalli grown from apical fragments, in WT, a *kar*<sup>KO</sup> mutant, and two representative *kar* complementation lines with the full-length KAR (*proKAR:C-KAR*) and with the PRONE domain (*proKAR:C-PRONE*) (Values are means  $\pm$  s.d.,  $n=4\sim 5$ ). Tukey's test was performed for the number of normal gemmae, and letters above the bars indicate significant differences at  $p < 0.05$ . Right panels show pictures of normal gemma of over 500  $\mu$ m diameter (normal), abnormal gemma with more than two notches, and small gemma of less than 500  $\mu$ m diameter.



**Figure 4. Expression of KAR and MpRop in vegetative tissues**

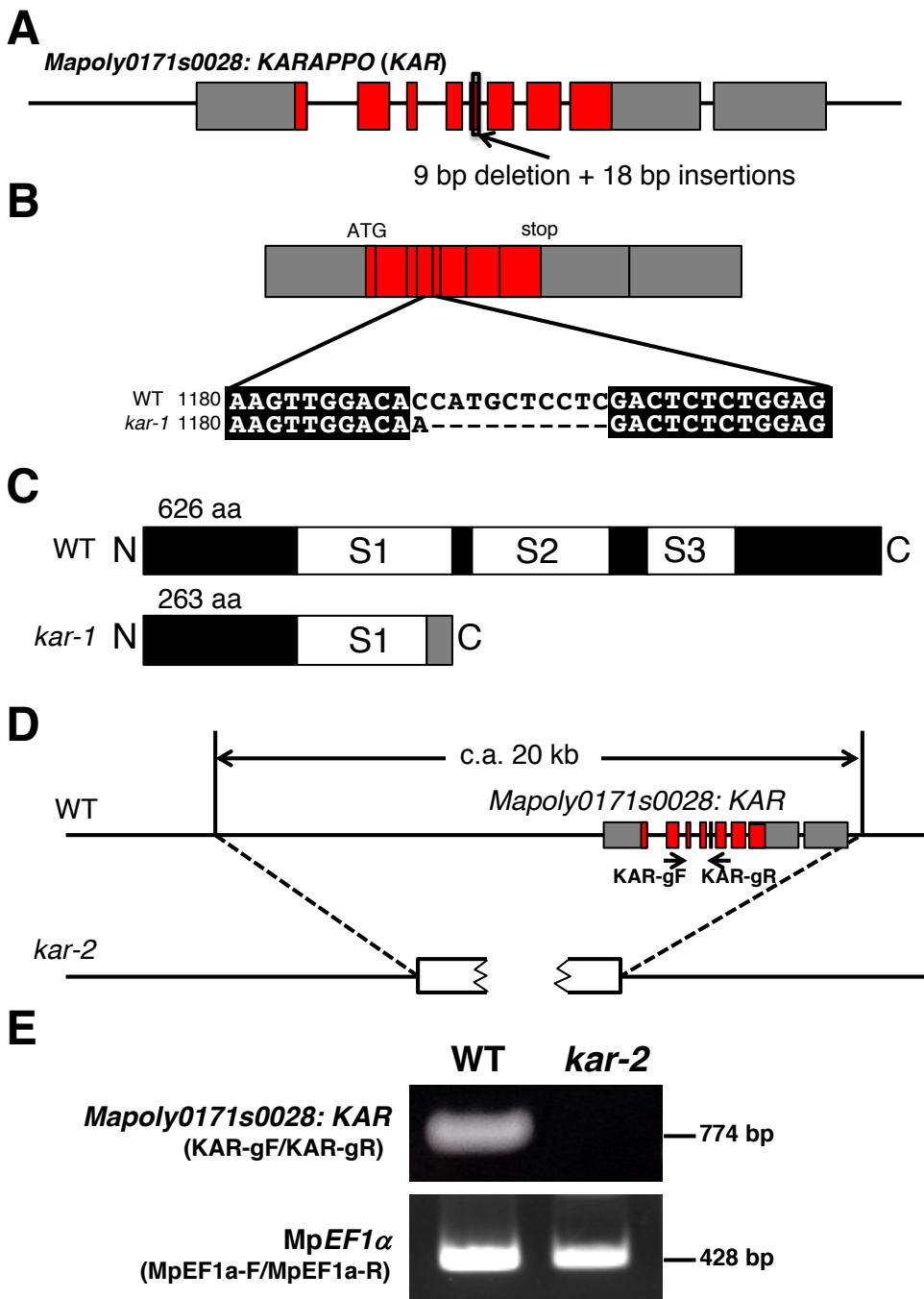
(A, B) Histological GUS activity staining of representative *proKAR:GUS* (A) and *proRop:GUS* (B) transgenic lines. (C) RT-qPCR analysis of *KAR* and *MpRop* in 1-week-old thalli yet to develop gemma cups (1w thallus), mature gemmae in gemma cups (gemma), gemma cups containing developing gemmae (gemma cups), and midribs. Total RNA was isolated from the respective tissues of Tak-1. *EF1α* was used as a control gene. Data are displayed as means  $\pm$  SD ( $n = 3$ ).

Figure S1-S4 and Table S1



**Figure S1. Gemma development in *M. polymorpha*, Related to Figure 1.**

(A) Optical observation of gemma and gemma cup in *M. polymorpha*. Gemma cups formed on the dorsal surface of gametophyte body, thallus. Top view of thallus (left), a close-up view of gemma cup (middle), and a transverse section of a gemma cup (right). (B-D) Electron microscopy in the basal floor of gemma cup. (B) Transverse section of a gemma cup. Red arrow-heads indicate developing gemmae. Blue-arrow heads indicate mucilage papillae. (C) Close up view of mucilage papillae observed at the floor epidermis of gemma cup. The right image shows an enlarged image of indicated cytosolic region in the left image. (D) Close up view of developing gemmae. Red arrows indicate basal stalk cells. (E) Schematic model of gemma development in the floor epidermis of gemma cup.



**Figure S2. Molecular characterization of *kar-1* and *kar-2*, Related to Figure 1 to 2.**

Whole genome analysis revealed respective mutations in *Mapoly0171s0028* locus in *kar-1* and *kar-2*. (A) Schematic representation of the *Mapoly0171s0028* genomic locus in wild-type and *kar-1*. Gray boxes indicate exons of untranslated region. Red boxes indicate exons of protein coding region. A small deletion found in the *Mapoly0171s0028* locus of *kar-1* genome. (B) cDNA sequences of *Mapoly0171s0028* in *kar-1*. (C) Schematic representation of deduced gene products of *Mapoly0171s0028* in wild-type and *kar-1*. (D) Whole genome analysis revealed c.a. 20 kb deletion in *kar-2*. Broken open boxes indicate partial fragments of pMT plasmid (Takenaka et al. 2000), which was introduced by particle bombardment protocol. A series of genomic PCR suggested that the 5' and 3' region of *Mapoly0171s0028* is not adjacent to each other in *kar-2* (data not shown), suggesting occurrence of a genomic rearrangement accompanied with the physical DNA delivery. (E) Genomic PCR of *Mapoly0171s0028* in wild-type and *kar-2*. *MpEF1 $\alpha$* ; *M. polymorpha* Elongation Factor alpha gene (*MpEF1 $\alpha$* ) was used as a positive control.

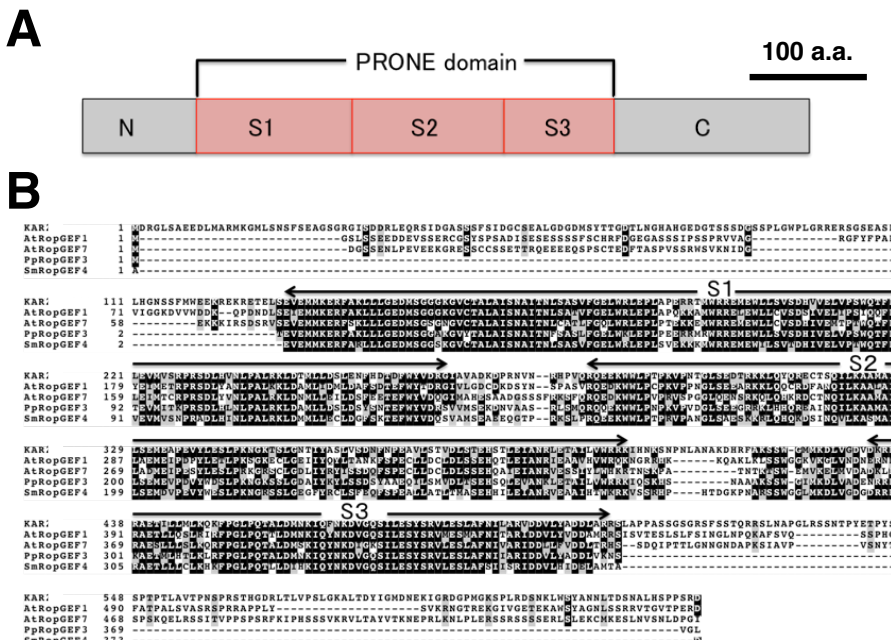


**Figure S3. KAR encodes a highly conserved PRONE domain of RopGEF, Related to Figure 2 to 3.**

(A) A domain structure of the *KAR* gene product. (B) Multiple alignment of the full amino acid sequences of KAR and representative RopGEFs in the moss *Physcomitrella patens*, the lycophyte *Selaginella moellendorffii* and *Arabidopsis thaliana* RopGEFs. Lines above aligned sequences indicate highly conserved regions in a PRONE domain composed of three subdomains (S1, S2, and S3), which has been in Arabidopsis to be essential for catalytic activity as guanine nucleotide exchange factor of ROP (Gu *et al.*, 2006; Oda *et al.*, 2012). (C) Unrooted Maximum-Likelihood tree of KAR and the other related RopGEF proteins across various plant lineages. The numbers on the branches show bootstrap values calculated from 1000 replicates. The scale bars are evolutionary distance at the ratio of amino acid substitutions.

**A**

```

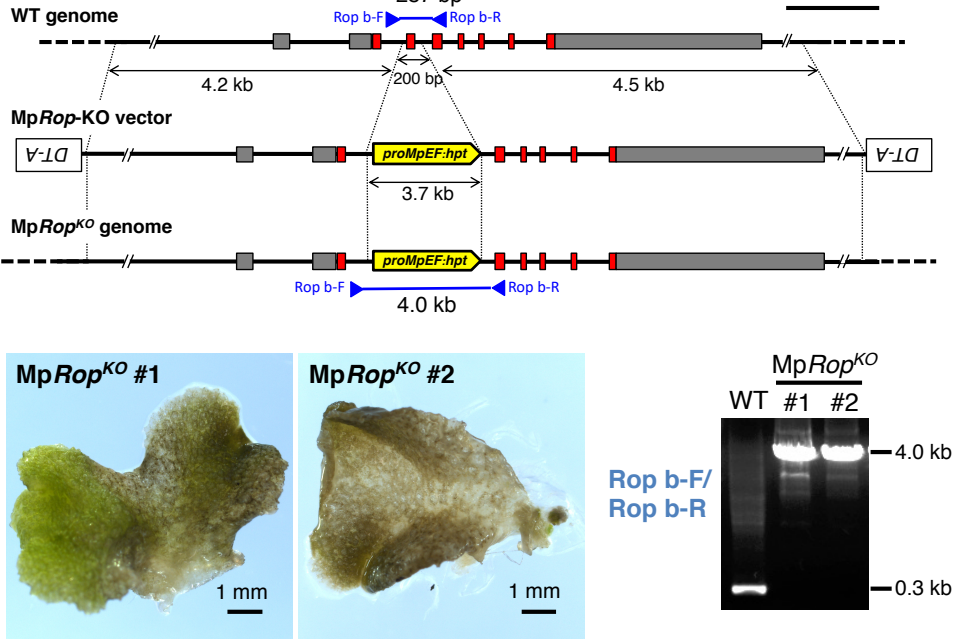
MpRop  1  M*SRFIKCVTVGDAVGKTCRLISYTSNTPTDYPVTFDNFSANVVVUGNTVNLLGLNDTAGQEDYNRLRPLSRYRGADVFLAFLSLKASYENISKWIPELRHYA
AtRop2  1  M*SRFIKCVTVGDAVGKTCRLISYTSNTPTDYPVTFDNFSANVVVUDGNTVNLLGLNDTAGQEDYNRLRPLSRYRGADVFLAFLSLKASYENISKWIPELRHYA
AtRop7  1  M*SRFIKCVTVGDAVGKTCRLISYTSNTPTDYPVTFDNFSANVVVUDGNTVNLLGLNDTAGQEDYNRLRPLSRYRGADVFLAFLSLKASYENISKWIPELRHYA
SmRop1 1  M*SRFIKCVTVGDAVGKTCRLISYTSNTPTDYPVTFDNFSANVVVUDGNTVNLLGLNDTAGQEDYNRLRPLSRYRGADVFLAFLSLKASYENISKWIPELRHYA
FpRop2 1  M*SRFIKCVTVGDAVGKTCRLISYTSNTPTDYPVTFDNFSANVVVUDGNTVNLLGLNDTAGQEDYNRLRPLSRYRGADVFLAFLSLKASYENISKWIPELRHYA

```

```

MpRop  111 VPIILVGKTKLDLRDKKFIDBPGAAPIITIQQEELKIGAMVIECSSKTQONVQAVFDAAIKVVLQPFQK-----KKKKQKTCV-----S-----
AtRop2  110 VPILVGKTKLDLRDKKFIDBPGAAPIITIQQEELKIGAMVIECSSKTQONVQAVFDAAIKVVLQPFQK-----KKKNKNRCAF-----S-----
AtRop7  111 VPILVGKTKLDLRDKKFIDBPGAAPIITIQQEELKIGAMVIECSSKTQONVQAVFDAAIKVVLQPFQK-----KKRSPICFFF-----S-----
SmRop1 111 VPILVGKTKLDLRDKKFIDBPGAAPIITIQQEELKIGAMVIECSSKTQONVQAVFDAAIKVVLQPFQK-----KKAKRRCCTV-----S-----
FpRop2 111 VPILVGKTKLDLRDKKFIDBPGAAPIITIQQEELKIGAMVIECSSKTQONVQAVFDAAIKVVLQPFQK-----KKKKQKCV-----XXXXX

```

**B***Mapoly0051s0092: MpRop***C**

|                       | RAC/ROP | RopGEF<br>(KAR) | SPK1 | REN | RopGAP | RopGDI | RIC | ICR |
|-----------------------|---------|-----------------|------|-----|--------|--------|-----|-----|
| <i>Arabidopsis</i>    | 11      | 14              | 1    | 3   | 5      | 3      | 11  | 5   |
| <i>Selaginella</i>    | 2       | 4               | 1    | 1   | 2      | 2      | 1   | 0   |
| <i>Physcomitrella</i> | 4       | 6               | 6    | 2   | 6      | 3      | 1   | 0   |
| <i>Marchantia</i>     | 1       | 1               | 1    | 1   | 1      | 2      | 0   | 0   |
| <i>Klebsormidium</i>  | 1       | 2               | 1    | 1   | 1      | 0      | ?   | 0   |
| <i>Chlamydomonas</i>  | 0       | 0               | 0    | 0   | 0      | 0      | 0   | 0   |
| <i>Ostreococcus</i>   | 1       | 0               | 1    | 0   | 0      | 0      | 0   | 0   |

**Figure S4. RopGTPase and its related gene families in *M. polymorpha*, Related to Figure 4**

(A) Multiple alignment of the full-amino acid sequences of MpROP and representative RopGTPases in *P. patens*, *S. moellendorffii*, and *A. thaliana*. (B) Generation of knockout mutants of MpRop. Schematic representation of the structure of the MpRop locus in wild type, the construct designed for gene targeting, and the MpRop locus disrupted in the gene-targeted lines (upper). Phenotype of two independent disruptants of MpRop gene showed severe impairment of thallus growth, and had died in the early stage of thallus development (lower left). A genotyping of MpRop indicates successful disruption of the cds structure occurred in MpRop knockouts (lower right). (C) Relative sizes of Rop signalling gene families in Viridiplantae. Total number of all homologous genes in the indicated gene families are indicated.

**Table S1. Oligonucleotide primers used in this study.**

| Name                | Sequence (5'→3')                               | Usage  |
|---------------------|--|--|
| kar-1_gF            | CCGTATTTGGAGAGTTGTGGA                          | genomic PCR of <i>kar-1</i>                              |
| kar-1_gR            | ACCGACTGCAGCTTGTGTT                            | genomic PCR of <i>kar-1</i>                              |
| KAR-gF              | CGGAAATTCTGCCTTCATGT                           | genomic PCR of <i>kar-2</i> and wild type                |
| KAR-gR              | CTCCAGCCTCCACAACCTCTC                          | genomic PCR of <i>kar-2</i> and wild type                |
| MpEF1a-F            | TCACTCTGGGTGTGAAGCAG                           | genomic PCR of <i>kar-2</i> and wild type                |
| MpEF1a-R            | GCCTCGAGTAAAGCTCGTG                            | genomic PCR of <i>kar-2</i> and wild type                |
| KAR_5IF_F           | CTAAGGTAGCGATTAATTAAATGAGCTTACCATATAATCACCGAGT | Construction of the targeting vector for KAR             |
| KAR_5IF_R           | GCCCGGGCAAGGTTAATTAAAGGTGGAACATTCTACATCGACAT   | Construction of the targeting vector for KAR             |
| KAR_3IF_F           | TAAACTAGTGGCCGCCGACCGGATACGAGTTCTTTCTT         | Construction of the targeting vector for KAR             |
| KAR_3IF_R           | TTATCCCTAGGCCGCCCTGGTAATCTCCAGAACCTCTGA        | Construction of the targeting vector for KAR             |
| a-F                 | TAGACTCGTAGTCTGGCCCTCAC                        | For checking of gene targeting site                      |
| b-F                 | GATGGGGACATGAGCTACACCAC                        | For checking of gene targeting site                      |
| b-R                 | CGAACCAACACGACGTCAGATT                         | For checking of gene targeting site                      |
| c-R                 | GTTGTGTGATTGTCGGGTAGAG                         | For checking of gene targeting site                      |
| P1R                 | GAAGGCTTCTGATTGAAGTTCTCTTCTG                   | For checking of gene targeting site                      |
| H1F                 | GTATAATGTATGCTATACGAAGTTATGTTT                 | For checking of gene targeting site                      |
| KARpro_GW_F         | GGCCAGTGCCAAGCTTACAACTGTGGCTCGACGAAC           | Construction of KARpro:KARcds                            |
| KARpro_GW_302_R     | TGTTGATAACTCTAGATCCATAGCCGAGCCACGTACAG         | Construction of KARpro:KARcds                            |
| KARpro_GW_305_R     | CCATGCTCATTCTAGATCCATAGCCGAGCCACGTACAG         | Construction of KARpro:Citrine-KARcds                    |
| KAR-cds-F           | caccATGGATCGAGGGCTCTGTCTG                      | Construction of entry clone containing KAR coding region |
| KAR-cds-sR          | CTAATCAGCACTGGAGGGCTGT                         | Construction of entry clone containing KAR coding region |
| PRONE_F             | CACCATGGAGGTCGAAATGATGAAGGA                    | Construction of KAR-PRONE entry clone                    |
| PRONE_R             | TCAAAGGAACGCTGGCTAAGTC                         | Construction of KAR-PRONE entry clone                    |
| MpRop_cds_F         | CACCATGAGTACTCCAGGTTAT                         | Construction of MpRop entry clone                        |
| MpRop_cds_sR        | TCACAGGATGGAACATGT                             | Construction of MpRop entry clone                        |
| KAR_WT_Y2H_pGADT7_F | GAGGCCAGTGAATTCatggatcgagggctctgt              | Constraction of Y2H vector                               |
| KAR_WT_Y2H_pGADT7_R | ACCCGGGTGGAATTCCtaatcacgactggagggtgt           | Constraction of Y2H vector                               |
| KAR_WT_Y2H_pGBK7_F  | ATGGAGGCCGAATTCatggatcgagggctctgt              | Constraction of Y2H vector                               |
| KAR_WT_Y2H_pGBK7_R  | GATCCCCCGGAATTCCtaatcacgactggagggtgt           | Constraction of Y2H vector                               |
| ROP_WT_Y2H_pGADT7_F | GAGGCCAGTGAATTCatgagtagttccaggttat             | Constraction of Y2H vector                               |
| ROP_WT_Y2H_pGADT7_R | ACCCGGGTGGAATTCtcacaggatgaaacatgtct            | Constraction of Y2H vector                               |
| ROP_WT_Y2H_pGBK7_F  | ATGGAGGCCGAATTCatgagtagttccaggttat             | Constraction of Y2H vector                               |
| ROP_WT_Y2H_pGBK7_R  | GATCCCCCGGAATTCtcacaggatgaaacatgtct            | Constraction of Y2H vector                               |
| KARpro_F            | CACCATACAACGTGGCTCGACGAAC                      | Construction of KARpro:GUS                               |
| KARpro_R            | ATCCATAGCCGACCCACCTACAG                        | Construction of KARpro:GUS                               |
| MpRoppro_F          | CACCTCCCTCGAGGATTTTCGAA                        | Construction of MpRoppro:GUS                             |
| MpRoppro_R          | AGTACTCATGTTCACTCCT                            | Construction of MpRoppro:GUS                             |
| PRONEcds_qRT-PCR_F  | AAGGAGAGGTTGCCCAAGC                            | RT-qPCR in Figure 3D                                     |
| PRONEcds_qRT-PCR_R  | TCTACCTCGAGGGCTTCAA                            | RT-qPCR in Figure 3D                                     |
| MpAPT-F             | CGAAAGCCAAGAACGCTACC                           | RT-qPCR in Figure 3D                                     |
| MpAPT-R             | GTACCCCCGGTTGCAATAAG                           | RT-qPCR in Figure 3D                                     |
| KAR-cds-F           | CACCATGGATCGAGGGCTCTGTCTG                      | RT-qPCR in Figure 4C                                     |
| KAR-gR              | CTCCAGCCTCCACAACCTCTC                          | RT-qPCR in Figure 4C                                     |
| MpRop_cds_F         | CACCATGAGTACTCCAGGTTAT                         | RT-qPCR in Figure 4C                                     |
| MpRop_cds_sR        | TCACAGGATGGAACATGT                             | RT-qPCR in Figure 4C                                     |
| MpEF1a-F            | TCACTCTGGGTGTGAAGCAG                           | RT-qPCR control in Figure 4C                             |
| MpEF1a-R            | GCCTCGAGTAAAGCTCGTG                            | RT-qPCR control in Figure 4C                             |
| MpRop_5IF_F         | ctaaggtagcgatTAAGGAGCTGGTTGAAGCCGAC            | Construction of the targeting vector for MpRop           |
| MpRop_5IF_R         | gccccggcaagcttATCAGTCAACAAGATCAAGGC            | Construction of the targeting vector for MpRop           |
| MpRop_3IF_F         | ttaaactagtggcgcgCACTAATTTCATCGTAT              | Construction of the targeting vector for MpRop           |
| MpRop_3IF_R         | ttatccctaggcgcgCACTGATCTTCACTCTCGTC            | Construction of the targeting vector for MpRop           |
| Rop_b-F             | GCCTCCAGTCGCCGTTCCGG                           | For checking of gene targeting site                      |
| Rop_b-R             | AGGAAACATCGGATGCCGGG                           | For checking of gene targeting site                      |